ELSEVIER

Chemical Engineering Journal 139 (2008) 172–193

Chemical Engineering Journal

www.elsevier.com/locate/cej

Review

Development of functionalized zeolite membrane and its potential role as reactor combined separator for *para*-xylene production from xylene isomers

Yeong Yin Fong, Ahmad Zuhairi Abdullah, Abdul Latif Ahmad, Subhash Bhatia *

School of Chemical Engineering, Engineering Campus, Universiti Sains Malaysia, Seri Ampangan, 14300 Nibong Tebal, Seberang Perai Selatan, Pulau Pinang, Malaysia

Received 17 July 2007; received in revised form 11 October 2007; accepted 17 October 2007

Abstract

Zeolite membranes are relatively new class of advanced materials where its characteristics have opened up the new opportunities of their application in separator, sensitive chemical sensors, and catalytic membrane reactor. The present review focuses on the development of functionalized zeolite membrane and subsequently its usage in the catalytic membrane reactor for combined separation and reaction of xylene isomers in a single unit. Synthesis of functionalized zeolite microporous crystal, development of functionalized zeolite membrane and xylene isomerization are presented and discussed. The models representing combined separation and reaction using functionalized zeolite membrane are also suggested.

Keywords: Functionalized zeolite membrane; Synthesis; Xylene isomerization; Catalytic membrane reactor; Modeling

1. Introduction

The industrial production and recovery of *para*-xylene is an important step in a large petrochemical plant. Xylene has three isomers namely *para*-xylene (molecular size ~0.58 nm), *ortho*-xylene and *meta*-xylene (molecular size ~0.68 nm) and are used as industrial solvents or intermediates for many derivatives [1–5]. Of the three xylene isomers, *para*-xylene has the largest commercial market. As reported by Ministry of Economy, Trade and Industry (MITE), Japan, the worldwide demand for *para*-xylene will increase to 27.8 million tonnes in year 2008 from 18.7 million tonnes in year 2002. *Para*-xylene is the feed for the production of pure terephthalic acid (PTA), which in turn is used in the production of polyester resin and fibers.

In order to meet the *para*-xylene demand, *para*-xylene is currently produced in the petrochemical industry through two different routes: (1) separation of *para*-xylene from its isomers and (2) conversion of less used *ortho*- and *meta*-xylenes to *para*-xylene through xylene isomerization reaction. Separation of *para*-xylene from its isomers is an important operation in the petrochemical industry, but it is difficult to separate the isomers due to their close boiling points, *para*-xylene (boiling point = 138.4 °C), *meta*-xylene (boiling point = 139 °C) and *ortho*-xylene (boiling point = 144.4 °C). Thus, the xylene isomers are currently separated by cryogenic crystallization, or selective adsorption process Parex, which is highly energy intensive. The current technology for xylene isomerization process such as XyMax (ExxonMobil) also consumes high energy. Therefore, there is a need to develop an efficient and energy saving technology to recover and separate *para*-xylene from its isomers.

Zeolite membranes or films have been in focus in recent years because of their well-defined micropore structure, good thermal and structural stability, high mechanical strength, feasible for steady-state operation, low energy consumption, resistance to relatively extreme chemical environment and great potential for combined steps of reaction/separation [2,6–10]. Zeolites are crystalline, microporous aluminosilicates which find extensive industrial usage as catalysts, adsorbents, and ion exchangers with high capacities and selectivities [9,11,12]. When zeolites are grown as films, zeolite membrane is formed. The characteristics of zeolite membrane have found its new application in gas, vapor and liquid separation especially in petrochemical industry based on their properties adsorption, preferential diffusion,

* Corresponding author. Tel.: +60 4 5996409; fax: +60 4 5941013.
E-mail address: chbhatia@eng.usm.my (S. Bhatia).

1385-8947/$ – see front matter © 2007 Elsevier B.V. All rights reserved.
doi:10.1016/j.cej.2007.10.019

Nomenclature

A	membrane area (m^2)
$[B]$	square matrix of inverse Maxwell–Stefan coefficients (m^{-2} s)
C_i	molar flow/concentration of component i (mol/m^3)
D_i	diffusion coefficients of component i (m^2/s)
E_i	activation energy for component i (kJ/mol)
H_i	sorption coefficients of component i (mol/m^3 Pa)
J_i	permeation flux of the component i (kg/m^2 s)
K_i	equilibrium constant
k_i	rate constant (s^{-1})
L	length of the reactor (m)
N_i	molar flux of component i (mol/m^2 s)
P	total pressure (Pa)
p_i	partial pressure of component i (Pa)
Q_i	volumetric flowrate of species i (m^3/s)
R_1	membrane radius on the retentate side (m)
$R_2 - R_1$	membrane radius on the permeate side (m)
r_i	rate of reaction of component i (mol/s kg_{cat})
$\Re$	ideal gas constant (J/mol K)
T	absolute temperature (K)
t	operating time (s)
W_i	weight of the component i (kg)
X	conversion
p	permeate
f	feed
x_i, y_i, z	molar fraction of component i at retentate, molar fraction of component i at permeate, the axial coordinate along the reactor length (m)

Greek letters

α	separation factor
$[\Gamma]$	matrix of thermodynamic factor
δ	membrane thickness (m)
Θ_i	molecular loading, molecules per unit cell or per cage
$\Theta_{i,sat}$	saturation loading, molecules per unit cell or per cage
$[\Theta_{i,sat}]$	diagonal matrix with the saturation loadings, molecules per unit cell or per cage
ν_i	stoichiometric coefficient of component i
ρ_z	density of zeolite (kg/m^3)
$\nabla\theta$	gradient of fractional loading

Subscripts

in	inlet
out	outlet
P	*p*-xylene
M	*m*-xylene
O	*o*-xylene

Superscripts

Pr	*p*-xylene in retentate
Pp	*p*-xylene in permeate
ir	*o*-xylene or *m*-xylene in retentate
ip	*o*-xyleneor *m*-xylene in permeate
r	retentate

or molecular sieving (size exclusion) [8,13–16]. Besides, membranes composed of different type of zeolites provide different framework structure and pore size, which make it suitable for application in membrane reactors, catalytic membrane reactor, sensitive chemical sensors, reactive and non-reactive gas sensors, electronic and thermoelectronic applications such as zeolite based capacitors [6,8,13,17]. Currently, zeolite membranes have been found of its promising applications in corrosion protection and antimicrobial coatings [18,19]. Table 1 shows the pore openings of different types of zeolites [20].

Among the zeolite membranes, zeolite MFI membranes (ZSM-5 and silicalite-1) are the most common membranes studied by the various researcher and thus, relative large information available for its synthesis and application in the literature. The pore structure of MFI zeolites are near to the sizes of many industrially important organic molecules, therefore its membrane can be used for the separation of organic compounds with kinetic diameters close to its pores. Zeolite MFI membrane has the pore structure of straight (*b*-oriented), circular pores (0.54 nm × 0.56 nm) interconnected with sinusoidal (*a*-oriented), elliptical pores (0.51 nm × 0.54 nm) and a tortuous path along the *c*-direction [1]. Fig. 1 shows the pore structure of MFI zeolite (ZSM-5 and silicalite-1).

One particular process in which zeolite membrane might offer significant advantage compare to existing technology is the separation of close-boiling point hydrocarbons, difficult to be separated by distillation or other complex and energy-intensive processes [1,12,21–24]. Thus, zeolite membrane offers potential application for the separation of xylene isomers in more effective way. As shown in Table 1 and Fig. 1, the pore structure of MFI zeolite is near to kinetic diameter of *para*-xylene, therefore its membrane can be used for the separation of *para*-xylene from its isomers.

In the recent years, researchers have explored the possibility of adding chemical functionalities to the pores of zeolites

Table 1
Aperture free diameter of selected zeolites [20]

Type of zeolite	Aperture free diameter (nm)
MFI (Zeolite Socony Mobil-5 or ZSM-5)	0.53 × 0.56
FER (Ferrierite)	0.35 × 0.48
FAU (Faujasite)	0.74 × 0.74
MOR (Mordenite)	0.65 × 0.70
MEL (Zeolite Socony Mobil-11 or ZSM-11)	0.53 × 0.54
BEA (Beta)	0.73 × 0.60
DDR (Deca-dodecasil 3R)	0.36 × 0.44
AFI (Aluminophosphate, AIPO-5)	0.73 × 0.73
AEL (Silicoaluminopihosphate SAPO-11)	0.39 × 0.63

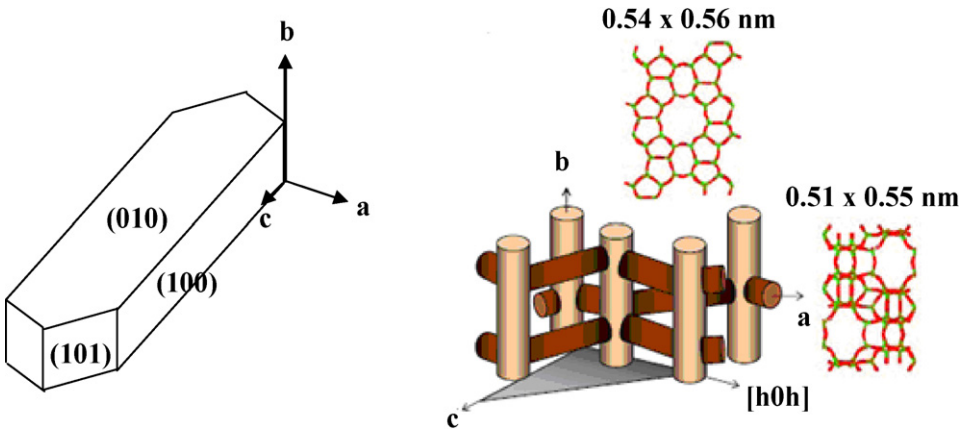

Fig. 1. Three-dimensional pore structure of MFI zeolite (ZSM-5 and silicalite-1).

with organic groups, result in organic-functionalized molecular sieves material which is crystalline with inorganic frameworks and pendant organic groups in the pores (Fig. 2). The synthesis of crystalline, microporous silicates (zeolite) with organic functionalities covalently adhered within the micropores resulted in new class of shape-selective catalysts with organic active sites. The organic functional groups confined within the micropores of the zeolites could be utilized as shape-selective catalysts for number of industrial important reactions [26–32]. These catalysts can be used in the synthesis of fine chemicals, pharmaceutical precursors and organic compounds.

The MFI zeolite membrane has a potential to perform as shape-selective catalysts for xylene isomerization when the organosulfonic acid groups are covalently attached to the framework of the zeolite crystals present in the membrane. Thus, the zeolite membrane could become an acid-functionalized zeolite membrane where the acidic functional group is the organic active reaction site for the isomerization reaction. The acid-functionalized zeolite membrane has strong acidity and hydrophilicity at elevated temperatures, molecular sieving capability, stable in most organic media and the active sites can be tailored to meet the needs of the reaction interest [26,30]. Therefore, acid-functionalized MFI zeolite membrane could be used as a catalytic membrane where the combination of xylene reaction and separation could be operated in a single reactive separation step. This type of process intensification may likely to increase the yield and production of *para*-xylene. At the same time, more efficient heat integration along with the simultaneous reaction and separation could be achieved in a single unit resulting in substantial savings.

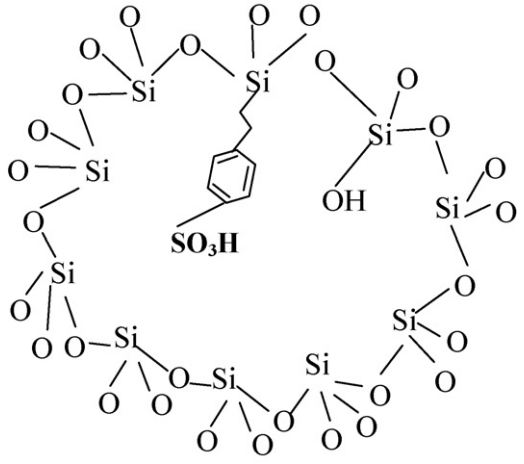

Fig. 2. Schematic micropore of acid-functionalized zeolite [25].

Synthesis and application of acid-functionalized MFI zeolite membrane where the acidic functional group is the organic active reaction site for the xylene isomerization reaction still remain a new task. Therefore, the present review is focusing on the potential development of acid-functionalized MFI zeolite membrane as a catalyst and separator (catalytic membrane reactor) for xylene isomerization process. The present review may lead to the better understanding of the process and factors responsible for the xylene isomerization and *para*-xylene separation over functionalized MFI zeolite membrane. The knowledge generated will be a first step leading to the development of catalytic membrane reactor to be used in the petrochemical industry for the production of *para*-xylene.

2. Zeolite membrane synthesis

Two critical stages are important to be considered during the formation of supported zeolite membrane: (a) nucleation and (b) crystal growth. These two stages are very sensitive to the experimental conditions such as synthesis solution/gel composition synthesis temperature, synthesis time and the supports which could be manipulated to control the crystal growth. The most common methods for synthesis of supported zeolite membranes reported so far are in situ crystallization, secondary (seeding) growth and vapor phase transport method (dry gel conversion method) [5,33]. Self-supported zeolite membranes have also been developed but of limited use because of their poor mechanical durability [4,13]. Template-free MFI zeolite membrane also being developed by Lin and coworkers [34], however, the effects of template on the pore opening of the membrane were not clearly discussed. It is clear that the preparation method influences the characteristics of the zeolite membrane formed especially of its microstructures and preferential orientation of the crystals [8].

2.1. In situ crystallization

In this method, a porous support is immersed in a synthesis mixture and the zeolite is allowed to crystallize during the hydrothermal treatment. During in situ synthesis method, zeolite nucleation is important. The zeolite crystal size, orientation and intergrowth depend on the numbers and types of nuclei formed on the support. The zeolite nuclei are formed either directly on the support by heterogeneous nucleation or deposited as embryonic seed crystals from the solution (homogeneous nucleation). The nucleation process is sensitive to the synthesis composition and temperature, the physicochemical properties of the support material and the presence of impurities. These characteristics make the nucleation process difficult to control, and may contribute to the poor reproducibility of the microstructure and the separation properties of the zeolites membrane [13,35,36].

2.2. Secondary growth

Tsapatsis and coworkers [1,37,38] proposed the secondary growth technique for the preparation of zeolite membranes. The secondary growth of a layer of zeolite seeds deposited on a support is currently recognized as one of the most attractive and flexible methods for the formation of membranes and films including A, L, Y, ZSM-5, and silicalite-1. Membrane growth from seeds provides better control of the membrane formation process by separating the crystal nucleation and growth, which results in short crystallization times [39]. The processing scheme consists of making a colloidal suspension of zeolite nanocrystals that are used to deposit a seed layer on a substrate. Few common methods have been practiced by the researchers to deposit zeolite seeds onto the substrate. The most common method for seed deposition is dip-coating. Vacuum seeding is another method where the seeding layer was closely attached to the support surface by the pressure difference between the two sides of the support wall [40]. Besides, electrophoretic deposition (EPD) has also been applied to coat the charged seeds onto the substrate [41]. By placing the seeded support in the synthesis mixture and treated under hydrothermal condition, the continuous oriented membrane will form by secondary grain growth of the deposited nanocrystals of the seed film. The elimination of the nucleation step, due to the presence of seed crystals on the support surface, provides improved flexibility for crystal growth and better control of film microstructure as well as enhanced reproducibility and scalability. Successful preparation and good separation properties of MFI zeolite membranes prepared by this technique have been demonstrated (refer to Table 2).

2.3. Oriented MFI zeolite membrane

The membrane performance is described by permeance/flux and separation factor are related to the membrane microstructure and orientation, for the application in gas or liquid separations. Therefore, the way to control the membrane microstructure and orientation is highly desirable. One of the challenging issue is the manipulation of the membrane orientation [14,36]. As shown in Fig. 1, *b*-oriented MFI films are of interest from the viewpoint of both fundamental study and practical application. Both experimental data and simulation results have suggested that the straight channel along the *b*-axis has the faster diffusion pathway in ZSM-5 crystal [14]. In addition to affecting the permeability, a preferred crystal orientation can cause differences in the stresses that affect the mechanical stability of the films [42]. Fig. 3 shows the oriented MFI crystal obtained by Lee et al. [43].

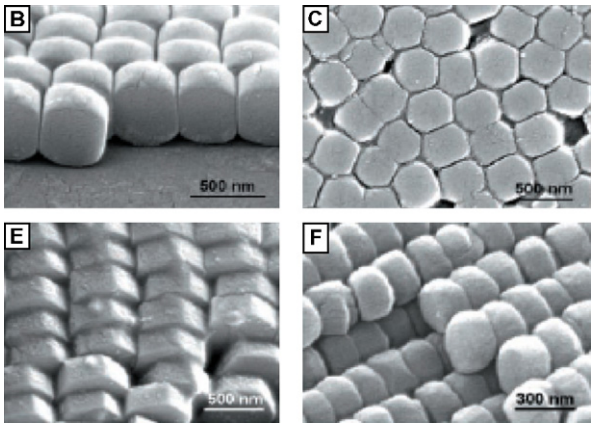

Fig. 3. SEM micrographs showing B, E, F: *c*-oriented and C: *b*-oriented silicalite-1 (MFI) crystal [43].

In the past few years, orientation MFI zeolite membrane has been reported by various researchers. These include Bons and Bons [44] ([*h* 0 *h*]-oriented), Wang and Yan [45] (*b*-oriented), Koegler et al. [46] (*ac*-plane), Exter et al. [42] (*a*, *b*-oriented), Dong and Long [47] [*h* 0 *h*] and *c*-oriented film). Effect of synthesis conditions on the orientation of the MFI zeolite membrane have been investigated and a growth model also has been purposed. Tsapatsis and coworkers [2] developed *c*- and [*h* 0 *h*]-oriented using secondary (seeded) growth method and its performance in xylene separation was studied. *b*-Oriented MFI membrane have also been successfully developed using modified secondary growth method [1,14]. This type of membrane has excellent performance in xylene separation.

Wang and Yan [45] reported the synthesis of *b*-oriented films on stainless steel supports using direct in situ crystallization. They studied the effect of crystallization temperature and time, surface roughness, position and chemical nature of the substrate, and the aging time of the synthesis solution and a mechanism for the *b*-oriented monolayer thin film formation was discussed. However, lack of flexibility of crystal growth and poor reproducibility of the oriented microstructure is suspected because of in situ crystallization method was used.

2.4. Modified secondary (seeded) growth for b-oriented MFI film

Recently, Tsapatsis and coworkers [1,14] developed a modified secondary (seeded) growth procedure that allowed to obtain *b*-oriented MFI zeolite membrane (refer Fig. 1), which showed excellent performance in xylene mixtures separation. In this method, a mesoporous silica layer coated onto the ceramic support by modifying the sol–gel technique developed by Brinker and coworkers [48] before the membrane growth. The role of

Table 2
Effect of synthesis parameters for development of oriented MFI zeolite membrane

Zeolite type	Gel composition	SDA	Synthesis method	Synthesis temperature and time	Support	Membrane thickness (μm)	Crystal orientation	Ref.
Silicalite-1	TEOS:0.23TPAOH:165H_2O	TPAOH	Secondary growth	175 °C, 8 h (two steps)	SS tube	25	*c*	[50]
Silicalite-1	1TEOS:*x*KOH:0.13Trimer-TPAI:238H_2O, $x = 0.20$ and 0.58	Trimer-TPAI	Modified secondary growth	175 °C, 24 h	SS 316L disk	Not given	*b*	[51]
Siliceous ZSM-5	40SiO_2:5Trimer-TPAOH:9500H_2O:8KOH:160EtOH	Trimer-TPAOH	Modified secondary growth	175 °C, 24 h	α-Al_2O_3 disc	1–1.5	*b*	[1,14]
	5SiO_2:1TPAOH:1000H_2O:20EtOH	TPAOH	Secondary growth	175 °C, 24 h	α-Al_2O_3 disc	12	*b*, *a*, *c*, *h* 0 *h*	
	5SiO_2:1TPAOH:1000H_2O:20EtOH	TPAOH	Secondary growth	90 °C, 5 days	α-Al_2O_3 disc	1.5–2	*b* and *a*	
Silicalite-1	TEOS:0.11TPAOH:110H_2O	TPAOH	Secondary growth	175 °C, 48 h	SS 316L disc	45	*c*, (*h* 0 *h*)	[52]
ZSM-5	TEOS:0.0175Al_2O_3:0.11TPAOH:110H_2O	TPAOH	Secondary growth	175 °C, 24 h	SS 316L disc	7.5	*c*, (*h* 0 *h*)	
Silicalite-1	40SiO_2:9TPAOH:9500H_2O:160EtOH	TPAOH	Secondary growth	140 °C, 96 h	α-Al_2O_3 disc	30	(*h* 0 *h*)	[9]
Silicalite-1	0.32TPAOH:TEOS:165H_2O	TPAOH	In situ crystallization	165 °C, 2 h	SS 304 plate	<0.4	*b*	[45]
Silicalite-1	4SiO_2:0.9TPAOH:950H_2O:16EtOH	TPAOH	In situ crystallization	140 °C, 20 h	α-Al_2O_3 disc	12–15	*a*	[53]
			Secondary growth				(*h* 0 *h*)	
Silicalite-1	0.84TEOS:0.23TPAOH:99H_2O	TPAOH	In situ crystallization	165 °C, 2 h	Silicon wafer	0.5	*b*	[42]
Silicalite-1	(5–20)TEOS:(0.41.5)TPA_2O:2000H_2O	TPAOH	In situ crystallization	180 °C, 4 days	Silicon	0.2–1	*a*, *c*	[46]
High-silica MFI seeds	R1·R2·Na_2O·SiO_2·H_2SO_4·NaF·H_2O·R1, R2 = EtHMTABr (*N*-ethyl-hexamethylenetetrammonium bromide), PA (*n*-propylamine), BA(*n*-butylamine) or EA (ethylamine)	Co-template, R1 and R2	In situ crystallization	160 °C for 5–30 days (or 180 °C for 2–15 days)	–	–	[1 0 0], [0 1 0]	[49]
		(i) EtHMTABr (*N*-ethyl-hexamethylenetetrammonium bromide) (ii) PA (*n*-propylamine) (iii) BA (*n*-butylamine) or (iv) EA (ethylamine)						

mesoporous silica layer is (1) to provide a smooth surface that can be functionalized for the deposition of the seeds, (2) to act as a barrier for avoiding zeolite deposit formation in the interior of the support and (3) to eliminate stress-induced crack formation during calcination at the support–zeolite interface. A silane coupling agent,3-chloropropyltrimethoxysilane, which has two functional groups, was used to covalently link seeds to the support. Trimer-TPAOH, structure-directing agent was used as zeolite crystal shape modifier to enhance relative growth rates along the *b*-direction. As a result, a thin, compact, crack-free, and *b*-oriented MFI membrane was successfully obtained. This microstructurally optimized film showed a significant improvement in separation performance for xylene isomers, as well as for other aromatic hydrocarbon mixtures.

2.5. Role of structure-directing agent (SDA)

Organic SDA's effects in zeolite synthesis are widely studied and the major role of SDA in the synthesis is inducing the formation of the zeolite with corresponding framework topography, known as template role [49]. Tetrapropylammonium hydroxide (TPAOH) and tetrapropylammonium bromide (TPABr) are the most often used structure-directing agent (SDA) in the synthesis of MFI zeolite membrane. However, formation of the randomly oriented zeolite membrane with low permeance and selectivities for xylene separation are also reported. Lai et al. [1] applied bis-*N*,*N*-(tripropylammoniumhexamethylene)di-*N*,*N*-propylammonium trihydroxide (trimer-TPAOH) as structure-directing agent which significantly enhanced the relative growth rate along the b axis and leads to of well-intergrown *b*-oriented ZSM-5 films on a porous support. Excellent separation performance of this membrane has been demonstrated on separation of *para*-xylene from *ortho*-xylene. The improved performance of the trimer-TPA-grown films could be attributed to (i) the preferential orientation of the straight channels, *b*-oriented film with small membrane thickness (ii) reducing the density of nonselective grain boundaries; and (iii) free of cracks and pinholes during calcinations [1,14]. The high-silica MFI-type zeolite crystals with *b*-axis orientation were hydrothermally synthesized using co-template (SDA) of *n*-propylamine *N*-ethyl-hexamethylenetetra-ammonium reactant system, by Yu et al. [49]. The co-template role for inducing the formation and the growth of *b*-axis oriented MFI zeolite crystals is discussed thoroughly in this paper.

2.6. Microwave (MW)-assisted hydrothermal synthesis

Motuzas et al. first demonstrated MW heating for the rapid synthesis of small and homogeneous silicalite-1 seeds and subsequently developed a controllable thickness, degree of crystallinity/orientation of silicalite-1 membrane [6,39]. They found that MW heating drastically shortens the synthesis duration time because long sol ageing (maturation–nucleation) times are not required. The influence of the chemical composition of the starting sol, the sol stirring time at room temperature and the hydrothermal synthesis conditions on the characteristics of the derived seeds have been widely studied. The hydrothermal synthesis parameters such as MW power, temperature, duration and number of synthesis steps have also been optimized in order to control the morphological characteristics and yield of the silicalite-1 crystals. Substantial efforts were made in order to synthesize thin silicalite-1 membranes by secondary growth from microwave-derived silicalite-1 seeds. The morphology, thickness, homogeneity, crystal preferential orientation (CPO) and single gas permeation properties of the silicalite-1 membranes have been studied in relation to the synthesis parameters [39]. Table 2 presents summary of synthesis parameters contributed for developing oriented MFI zeolite membrane. As shown in Table 2, silicalite-1 zeolite membrane is preferentially oriented compared to ZSM-5 zeolite membrane and most of the ZSM-5 membrane synthesized are randomly oriented.

3. Xylene separation using zeolite membrane

An extensive study of xylene separation using zeolite membrane especially MFI membrane was performed by various researchers in the past few years [1,2,4,5,13–16,34,54–56]. As reported in the literature, it is crucial to know how to prepare zeolite membranes with high permeability and selectivity. Although many different strategies have been employed, the synthesis of these type of membrane imposes challenges such as control of thickness, grain size, crystal orientation, minimization of the effect of grain boundary defects (such as channel blockages or intercrystalline paths with openings that are larger than the zeolite pores) and avoiding stress-induced crack formation during membrane synthesis [1].

MFI zeolite membrane with the desired microstructure has superior performance for the separation of organic mixtures especially for xylene isomers. It was found that *b*-oriented MFI zeolite membrane gave the best results in term of flux and separation factor for the separation of *para*-xylene from its isomers. Beside the membrane quality, the influence of operating conditions especially temperature and feed concentration are the major factors contributed to the separation behavior of the xylene mixture. Two different processes which are used to separate *para*-xylene from its isomers:

(i) Vapor permeation (VP)
   - The feed mixture is in the vapor form.

(ii) Pervaporation (PV)
   - The feed mixture is in the liquid form.

Table 3 presents the permeance or flux and separation factor (selectivity) results in the separation of xylene mixture using zeolite membrane; with vapor permeation and pervaporation reported by the various researchers in the literature.

Different suggestions have been made by the various researchers based on the results achieved in xylene mixtures separation. Keizer et al. [15] obtained separation factors of *p*-xylene/*o*-xylene <1.0 at 298 K and >200 at 375–415 K, for 0.31 kPa *p*-xylene and 0.26 kPa *o*-xylene binary mixture showing that the separation factors were significantly dependent on the operating temperature. The membrane showed a possibility

Table 3
Separation factor and permeance results obtained by various researcher on xylene separation using MFI zeolite membrane

Zeolite type	Crystal orientation	Membrane thickness (μm)	Operating temperature (°C)	Feed partial pressure (kPa)	Separation factor (binary mixture)	Permeance (mol/m^2 s Pa)	Ref.
Silicalite-1	Random	2	250	*p*-X = 0.52 *o*-X = 0.39	17.8	*p*-X = 9.5×10^{-9} *o*-X = 6.0×10^{-10}	[56]
			250	*p*-X = 0.26 *o*-X = 0.20 *m*-X = 0.49	*p*/(*m* + *o*) = ∼30 *p*/*m* = ∼30 *p*/*o* = ∼30	*p*-X = 1.1×10^{-8} *o*-X = 4.2×10^{-10} *m*-X = 4.2×10^{-10}	
Silicalite-1	*c*	25	150	*p*-X = 0.23 *o*-X = 0.26 *m*-X = 0.83	*p*/*m* = 4.6 *p*/*o* = 3.6	*p*-X = 7.5×10^{-6} mol/s.m^2 *o*-X = 6.5×10^{-7} *m*-X = 2.6×10^{-6}	[50]
*Siliceous ZSM-5	*b*[0 *h* 0]	1	200	*p*-X = 0.45 *o*-X = 0.35	500	*p*-X = 2.00×10^{-7} *o*-X = 7.00×10^{-10}	[1]
Siliceous ZSM-5	*a* and *b*	1	180	*p*-X = 0.45 *o*-X = 0.35	3	*p*-X = 2.00×10^{-7} *o*-X = 1.00×10^{-7}	
MFI	Random	0.5	100	*p*-X = 0.30 *o*-X = 0.25	3.2	*p*-X = 6.00×10^{-7}	[11]
			390	*p*-X = 0.30 *o*-X = 0.25	16	*p*-X = 3.00×10^{-7}	
ZSM-5 high Si/Al = 360	Random	60–90	200	*p*-X = 0.3	*p*/*o* = 250	*p*-X = 8.00×10^{-8}	[4]
				o-X = 0.27 *m*-X = 0.27	*p*/*m* = 250	*o*-X = 1.00×10^{-9} *m*-X = 1.00×10^{-9}	
Silicalite-1	[*h* 0 *h*]	2 to 3	125	*p*-X = 0.45 *o*-X = 0.35 *p*-X = 0.9 (single) *o*-X = 0.7 (single)	12	*p*-X = 2.25×10^{-8} *o*-X = 3.13×10^{-10} *p*-X = 3.75×10^{-8} *o*-X = 3.13×10^{-9}	[2]
Silicalite-1	Random	–	127	*p*-X = 2.1 *o*-X = 2.1	4.6	*p*-X = 1.20×10^{-9} *o*-X = 2.40×10^{-10}	[16]
ZSM-5	Random	–	177	*p*-X = 2.1 *o*-X = 2.1	5.5	*p*-X = 1.90×10^{-9} *o*-X = 2.40×10^{-10}	
Boron substitute ZSM-5 (B-ZSM-5)	Random	–	132	*p*-X = 2.1 *o*-X = 2.1	60	*p*-X = 5.60×10^{-11} *o*-X = 9.30×10^{-13}	
Silicalite-1	Random	3	125	*p*-X = 0.31 *o*-X = 0.26	>200	*p*-X = 1.05×10^{-8} *o*-X = 1.75×10^{-11}	[15]
			200	*p*-X = 0.31 *o*-X = 0.26	30	*p*-X = 1.05×10^{-8} *o*-X = 1.75×10^{-10}	
Silicalite-1 template-free	Random	3 to 5	50 (PV)	Equimolar binary mixture	40	*p*-X = 0.137 kg/m^2.hr *o*-X = 0.003 kg/m^2.hr	[34]
Al-free ZSM-5	Random	1.5	26 to 75 (PV)	Equimolar binary mixture	1	*p*-X = 8.80×10^{-9} *o*-X = 7.00×10^{-9} *m*-X = 1.03×10^{-8}	[54]

of the separation of a mixture of xylene isomers with the MFI membranes in vapor permeation.

Gump et al. [16] investigated the xylene isomers separation using SAPO, MOR, randomly ZSM-5, silicalite-1 and boron substitutes ZSM-5. They found that boron substitutes ZSM-5 membrane had highest separation factor of 60. The substitution of boron in the framework reduced the loss of selectivity, possibly by decreasing the unit cell size and making the framework more rigid. The SAPO membranes exhibited single-file diffusion and, therefore, no separation selectivity. MOR membrane was unable to separate the aromatics, possible because of the smaller role of adsorption and pore blocking at the higher temperatures and the lower feed concentration of the vapor permeation experiments.

Sakai et al. [4] studied self-supporting MFI-type zeolite membrane, in order to avoid the defect formation due to the thermal expansion mismatch between alumina support and zeolite membrane during calcination. The separation of ternary mixtures of xylene isomers was performed between 303 and 673 K, feed partial pressure between 0.3 and 5.1 kPa. The separation fac-

tors of *p*-xylene to *m*-xylene and *p*-xylene to *o*-xylene showed the maximum value of 250 at 473 K. In 2002, the first example of high-pressure, high-temperature gas separation of xylenes was carried out at 673 K and100 kPa hydrocarbon partial pressure (200 kPa total pressure), using MFI zeolite membrane by Hedlund et al. [11].

Xomeritakis et al. [2] investigated the separation of xylene isomer vapors with oriented MFI membrane in the temperature range of 22 °C (295 K) to 275 °C (548 K) and feed partial pressure up to 0.7–0.9 kPa. They found that the separation performance of these membrane was directly related to the synthesis conditions and the resulting membrane microstructure. *c*-Oriented membrane exhibited single component *p*-xylene/*o*-xylene permselectivity as 150 and modest separation factor of <5 at temperature of 373 K was obtained for binary mixtures. (*h* 0 *h*)-oriented membrane exhibited comparable single component and binary permeation behavior but lower separation factor of 12 if compared with *b*-oriented membrane, due to the formation of cracks during template removal after calcinations.

Recently, Gu et al. [56] investigated the separation of *p*-xylene from *m*-xylene and *o*-xylene in binary, ternary, and simulated multicomponent mixtures over wide ranges of feed pressure and operating temperature, using MFI zeolite membrane. Tarditi et al. [50] used silicalite-1 and ZSM-5 films supported on porous stainless steel tubes to investigate separation of xylene isomers between 150 and 400 °C (673 K). Permeation measurements of the individual isomers and the ternary mixture were performed at each temperature within this interval. They found that ZSM-5 membrane was superior to the silicalite-1 one because of its higher permeance flux (1.16×10^{-5} mol/s m^2), separation factors (*p*/*o* 4.4), and up to 400 °C (673 K) stability.

Pervaporation of pure xylene isomers and their binary mixtures through MFI zeolite membrane has been studied by Wegner and coworkers [54]. They found that intensive fouling of the zeolite membrane was observed during the pervaporation experiment due to strong interaction of xylene molecules with the zeolite pores, although the membrane permeable for all xylene isomers. However, no separation of binary *p*-xylene/*m*-xylene and *p*-xylene/*o*-xylene mixtures could be obtained in the temperature range 26–75 °C (299–348 K) studied.

Template-free silicalite-1 zeolite membrane with minimum intercrystalline pores and excellent performance of the membrane for separation of xylene isomers by pervaporation has been reported by Yuan et al. [34]. Separation performance for pure and binary xylene mixtures has been tested by using the silicalite-1 zeolite membranes synthesized by using template and without using template. The best pervaporation separation result in term of flux and selectivity for xylene separation was reported for template-free silicalite-1 membrane with the separation factor of *p*-xylene/*o*-xylene as 40.

Tsapatsis and coworkers [1,14], reported the best result of MFI-type zeolite membranes for vapor permeation separation of xylene isomers. The *b*-oriented zeolite membrane was obtained by a secondary growth method with a *b*-oriented seed layer and use of trimer-TPA as a template in the secondary growth step. The membrane gave *p*-xylene permeance about 2×10^{-7} mol/m^2 s Pa with *p*-xylene/*o*-xylene separation factor up to 500. The zeolite crystal orientation and the thickness of the membrane play a key role in determining the performance of zeolite membranes in xylene separation.

4. Functionalized zeolite microporous crystal: organic–inorganic hybrid material

During the last decade, functionalized nanoparticles with organic groups have been prepared. These include metal oxide nanoparticles of various chemical compositions, structures and properties, for example silica, titania and zirconia, were functionalized and used for different purposes. Since the discovery of the M41S class of mesoporous silicates, incorporation of organic groups to impart functionalities to the pore surface of the mesoporous silica materials has attracted much attention due to the potential applications of the resultant materials in the field of catalysis, separation, sensor design, and nanoscience [57]. However, the weak hydrothermal stability of these mesoporous organosilica materials prepared by conventional methods limits their practical and potential applications.

The introduction of organic groups into an inorganic network of zeolite pore leads to new variation of structural property, thereby promoting new potential applications for the resulting hybrid materials [58,59]. These microporous hybrid solids show structural short-range order and a homogeneous and regular pore distribution, which favor molecular sieving effects. The combination of inorganic and organic fragments inside the structure of porous zeolitic materials can give rise to new organozeolites preserving the positive characteristics of both organic and inorganic materials, which will greatly broaden their usefulness [58].

Microporous molecular sieves containing intracrystalline organic functionalities covalently adhered to framework silicon atoms provides for the possibility of performing shape-selective catalysis with inorganic solids containing organic active site [27]. Therefore, the solid catalyst, acid-functionalized zeolite crystal, has been the subject of many researchers because of safety, low cost and ease of recovery derived from the heterogeneous catalysis [30]. Besides, the functionalized zeolite nanoparticles were envisaged for the preparation of controlled release capsules, artificial cells, chemical sensors and adsorbents [29]. The modification of such materials by organic functional molecules will also greatly broaden their usefulness [31].

4.1. Pore size modification: organic-functionalized zeolite crystal

The first synthesis of a shape-selective organic-functionalized molecular sieve (OFMS) was reported by Jones et al. [26]. Zeolite and related microporous crystalline molecular sieves containing organic functionalities within their pores have been synthesized, which possess catalytically active acid sites with uniform size and shape pores and voids. They reported a new methodology that allows the production of a wide range of shape-selective catalysts where the different active site types could be generated by attaching other functional groups to the framework silicon. The synthesis of crystalline, organic-

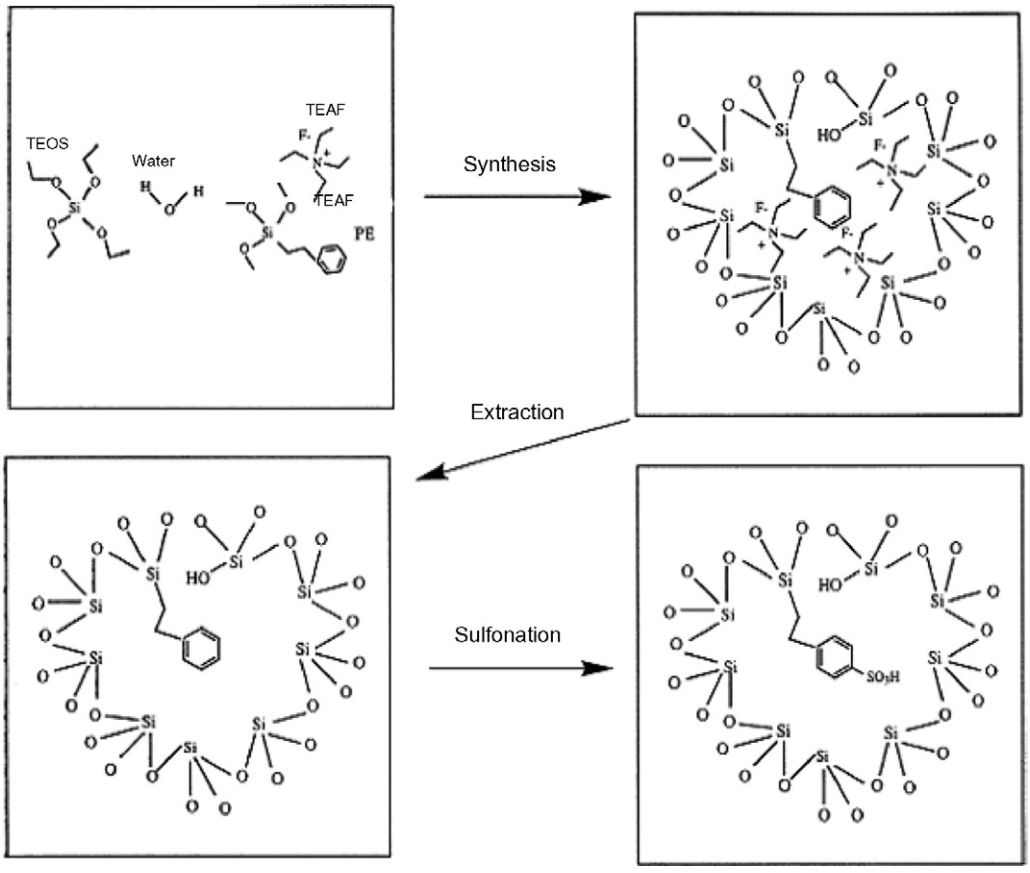

Fig. 4. Synthesis strategies of OFMS with non-polar organic groups, phenethyltrimethoxysilane (PE) [26].

functionalized molecular sieves having beta (BEA) topology where the polar functional group, an aminopropyl, covalently adhered within the micropores has been achieved. Their results indicate that the aminopropyl groups are located within the intracrystalline void space and that they can be reacted with aldehydes to form occluded imines [26,28].

Subsequently, the detailed synthesis and characterization of OFMSs containing non-polar functional groups, phenethyl (PE) has been demonstrated. The phenethyl groups were sulfonated to produce a microporous solid containing intracrystalline sulfonic acids, which was transformed into solid catalyst. These materials have shown to be an effective shape-selective catalyst for various reactions based on organic active sites, as the active site can be tailored to meet the needs of the reaction interest. Fig. 4 shows the synthesis strategies of OFMS with BEA topology using two different route, which was described by Jones et al. [26].

Non-polar functional groups such as ethylcyclohexenyl (CHE) and mercaptopropyl (MP) have been used in the synthesis of acidic OFMSs with the beta (BEA) topology by Jones et al. [27]. These acidic OFMSs were investigated for use as shape-selective catalysts for the conversion of cyclohexanone relative to 1-pyrenecarboxaldehyde. Their results show that sulfonic acid containing OFMSs derived from the oxidation of mercaptopropyl(MP) groups were very selective for the conversion of cyclohexanone relative to 1-pyrenecarboxaldehyde (PYC). Acidic OFMSs based on oxidized MP groups showed good shape-selective properties although their activities are low. The shape-selective catalytic activity for sulfonic acid, mercaptopropyl silane zeolite beta was further confirmed by Shin et al. [31]. They reported that major SO_3H groups reside inside the zeolite pore channels and act as the active center for the reaction. Table 4 shows the molecular structure of functional groups studied by Jones and coworkers [26–28].

Fig. 5 shows the SEM micrograph of organic–inorganic hybrid zeolites containing an organic group as lattice (ZOLs) reported by Yamamoto et al. [60]. The characterization results show that both ZOL-1 (MFI-type) and ZOL-B (BEA-type) materials structures were retained after the calcinations at 540 °C (~73% for ZOL-B).

Different types of microporous hybrid organic–inorganic materials with ITQ-21, MFI and BEA structures have also

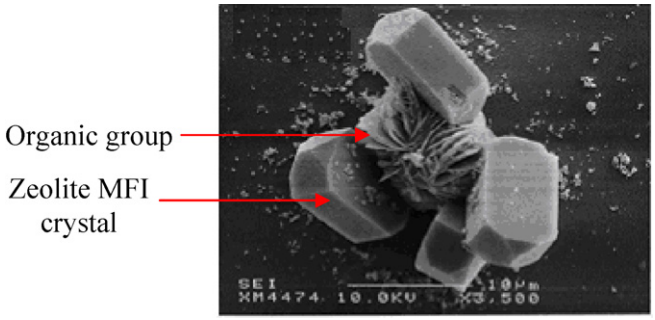

Fig. 5. SEM images of ZOL materials [60].

Table 4
Molecular structure of functional groups introduced into the zeolite pores [26–28]

Functional group	Molecular structure
Phenethyl (PE) trimethoxysilane	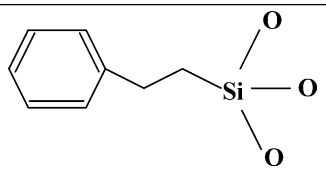
Mercaptopropyl (MP) trimethoxysilane	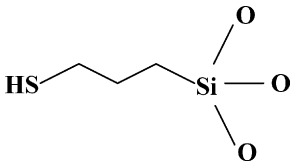
Ethylcyclohexenyl (CHE) trimethoxysilane	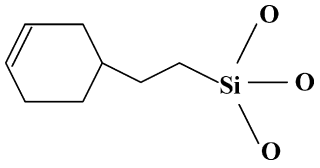
2-(3-Cyclohexenylethyl) trimethoxysilane	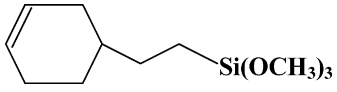
3-Butenyltriethoxysilane	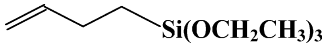
3-Mercaptopropyl-trimethoxysilane	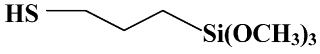

been synthesized from bridged organosiloxane precursors as silica sources by Diaz et al. [58]. Their results showed that the organic–inorganic networks were thermally stable and remained stable after elimination of the structure-directing agents (SDAs) by calcinations. The characterization techniques confirmed the incorporation of organic fragments into the framework, bonded covalently to other inorganic units to conform a true hybrid organic–inorganic structure.

The functional groups such as phenethyl (PE) trimethoxysilane, mercaptopropyl (MP) trimethoxysilane and ethylcyclohexenyl (CHE) trimethoxysilane could be introduced into the zeolite pore and subsequently oxidize to acid-functionalized zeolite membrane; which can be used as acid catalyst for xylene isomerization process. The potential for development of this type of material is further discussed in the following section.

4.2. Synthesis of acid-functionalized zeolite crystal

Four different methods have been successfully applied by various researchers for synthesizing of organic-functionalized zeolite crystals, i.e. post-synthesis grafting [25,57,59], in situ deposition [57,59], grafting using supercritical fluid silanation process ($SCCO_2$) [31] and two consecutive grafting procedures [29]. For post-synthesis grafting method, the functional groups are grafted onto the surface of the zeolite particles by repeated centrifugation and re-dispersion under ultrasonification. In situ deposition is the most common method used by the researchers where the functional groups are presented in the synthesis gel as silica source. Grafting using supercritical fluid silanation process is a method where supercritical carbon dioxide is used to deposit functional group into the microporosity of zeolite pores. Two consecutive grafting procedures are generally used. Firstly, the functional groups grafted at template-containing zeolite nanocrystals inhibit irreversible aggregation during the combustion of the structure-directing agent. Secondly, grafting provides stable colloidal functionalized zeolite nanocrystals with organic ligands grafted at silicon or aluminium surface zeolite atoms. Comparatively, the direct synthesis pathway by co-condensation of siloxane and organosiloxane precursors often offers a better control of the resultant materials in terms of a higher and more uniform surface coverage of the organic functionalities without the blockage of the pores [57]. However, to synthesize acid-functionalized zeolite crystal, acid treatment (post-treatment) is applied. The functional groups are sulfonated to produce a microporous solid containing intracrystalline sulfuric acid (acid-functionalized zeolite crystals) which are transformed to acid catalyst. Table 5 lists the functional groups commonly used by the researchers and the

Table 5
Functional groups and synthesis methods for functionalized zeolite

Functional groups	Synthesis method	Post-treatment (functional group)	Structure	Ref.
Phenethyltrimethoxysilane (PE)	In situ deposition	Sulfonation	Zeolite beta and MCM-41 mesoporous silica	[26,27]
	In situ deposition	Sulfonation	Zeolite beta	[30]
Mercaptopropyltrimethoxysilane (MP)	In situ deposition	Sulfonation	Zeolite beta and mesoporous silica	[27,32]
Ethylcyclohexanyltrimethoxysilane (CHE)	In situ deposition	By contact the ethylcyclohexenyl-functionalized crystals with bromine vapor for 2–3 h	Zeolite beta	[27]
Tris(methoxy)mercaptopropylsilane (TMMPS)	Grafting using supercritical fluid silanation process ($SCCO_2$)	-TMMPS groups were oxidized with 30% aqueous H_2O_2 dissolved in methanol for 24 h -The oxidized materials were resuspended in 15 ml of H_2SO_4	Zeolite beta	[31]

methods applied in the synthesis of acid-functionalized zeolite crystals.

4.3. Synthesis of functionalized zeolite: current problems

Functionalized zeolites is a new type of materials having a large potential as a shape-selective catalyst as well as other application, depending on the functional group. Organic functionalization of zeolites would widen the range of their applications because of larger organic contents in the zeolites material are of special interest in catalysis, adsorption, storage and nanotechnological fields, making use of mechanical, optical, electronic and magnetic properties provided by the structural organic fragments [58]. The organic functional groups can be easily chosen and designed to meet different requirements, but up to date, only a number of the organic functional groups could be introduced through the direct co-condensation (in situ deposition) method [57]. Some of the problems existing for development of organic-functionalized zeolite include:

- Amorphous impurities; future studies should aim to remove this trace amorphous impurity, in order to obtain highly crystalline OFMS materials.
- The use of organosilanes with pendant organic groups has inevitably led to structural defects, and organic groups located in micropores may spoil the microporosity.
- The pores could be blocked by the organic functional groups (only high-silica zeolites were prepared).

Another critical problem was the exterior surfaces deposition of the functional group of the crystals, as pointed out by Jones et al. [27]. They found that in the post-synthesis deposition (grafting), a large fraction of the organosilanes is deposited in the exterior surface of the materials and subsequently no size selectivity has been observed. Besides, the distribution of the functional groups on the surface of the pore wall is likely not uniform although the resultant materials maintain highly ordered structures and show relatively high hydrothermal stability after grafting reaction.

Therefore, further studies are needed to overcome the existing problems for synthesis this type of material. It is known that organic-functionalized zeolites can perform as acid/base shape-selective catalyst; depending on the organic functional group. Thus, selection of organic functional group is a very important step based on the type of reaction studies. There is need to find the suitable organic functional group for specific reaction, together with the optimum functional group need to be deposited inside the pore to maximize the reaction rates. In order to overcome the problems of pore blocking by organic functional group, exterior deposition, low crystallinity and uneven distribution of organic group in the zeolite pores, an improvement in the synthesis methodology need to be explored.

5. Xylene isomerization

Xylene isomerization is a well-known acid-catalyzed reaction and most of the currently xylene isomerization plants are using zeolite based catalysts like HZSM-5. On acid zeolite catalysts, *m*-xylene undergoes two competitive transformations, isomerization into o-xylene and *p*-xylene and disproportionation into toluene (T) and trimethylbenzene (TMB), as shown in Fig. 6 [26,39,61–65]. Isomerization of *m*-xylene involved monomolecular or intramolecular mechanism while disproportionation of *m*-xylene involved bimolecular or intermolecular mechanism. The formation of *o*-xylene and *p*-xylene by converting a *m*-xylene rich industrial feed can be adequately described by the monomolecular mechanism including a 1,2-methyl group shift [62,66–69].

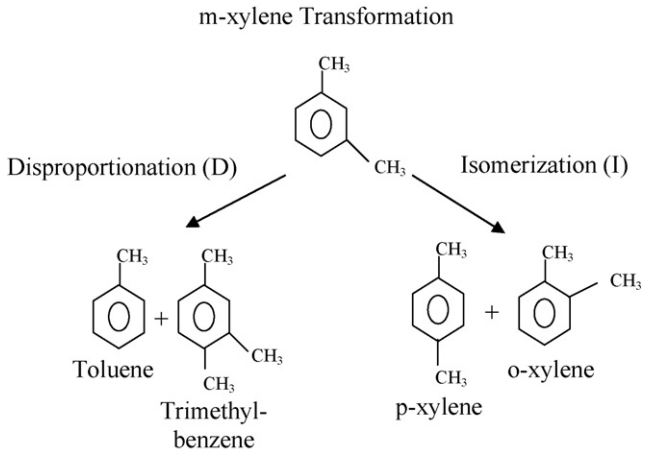

Fig. 6. *m*-Xylene transformation.

Xylene isomerization is generally carried out in a fixed bed reactor [25,61,64,70]. Catalytic membrane reactor [21,67], in situ flow cell (CSTR) [71], riser simulator reactor [66] and fixed bed microreactor [69] using zeolite catalyst are also reported in order to obtain the higher yield of *p*-xylene. Table 6 shows the use of zeolite catalyst for xylene isomerization studies. The factors affecting the conversion, reactant diffusion, products selectivity and reaction pathways during isomerization of xylene are

- acidity of the zeolite catalyst [26,62,66,67,71,72];
- pore size (shape-selective property) of the zeolite catalyst [26,63,65];
- operating parameters (e.g. temperature).

Thus, optimizations of these factors are needed to minimize disproportionation in favor of isomerization reaction, especially to *para*-isomer. A proper study on the contribution of zeolite membrane acidity and pore size modification on the performance of zeolite membrane are crucial in xylene isomerization reaction.

6. Development of functionalized zeolite membrane for combined xylene isomerization and separation

For the development of catalytic functionalized zeolite membrane reactor for combined xylene separation and isomerization, silicalite-1 membrane has been chosen. In order to develop functionalized zeolite membrane, zeolite membrane with pure silica form is needed. However, silicalite-1 is an aluminum-free ana-

Table 6
Xylene isomerization studies using zeolite catalyst

Catalyst	Type of reactor	Feed	Activity	Operating temperature (°C)	Remarks	Ref.
HZSM-5	Catalytic membrane reactor	*p*-Xylene, *m*-xylene, *o*-xylene	Increase 15% of *m*-xylene conversion compare to packed-bed reactor conversion = 4–17%	355–450	–	[67]
Pt/HZSM-5	Fixed bed microreactor	Industrial *p*-xylene-depleted xylene feedstock (10 wt.% ethylbenzene, 10 wt.% *p*-xylene, 20 wt.% *o*-xylene, 60 wt.% *m*-xylene	Formation of toluene: 0.99 wt.%	300–400	Catalyst pore size of 0.535 nm and 26% strong acid site	[69]
Pre-coking			0.78 wt.%		Catalyst pore size of 0.538 nm and 3% strong acid site	
Silanization			1.01 wt.%		Catalyst pore size of 0.505 nm and 21% strong acid site	
HZSM-5	Microreactor chromatograph technique	*p*-Xylene, *m*-xylene, *o*-xylene	At 513 °C, conversion: *p*-Xylene = 79.95% *m*-Xylene = 40.80% *o*-Xylene = 1.10%	396–513	Catalyst with 2.90 strong acid site/unit cell	[65]
MgO-HZSM-5			*p*-Xylene = 75.20% *m*-Xylene = 30.15% *o*-Xylene = 28.26%		Catalyst with 0.80 strong acid site/unit cell	
CaO-ZSM-5			*p*-Xylene = 78.22% *m*-Xylene = 27.32% *o*-Xylene = 27.03%		Catalyst with 0.65 strong acid site/unit cell	
HFAU (HY)	Fixed bed reactor	*m*-Xylene	-Greater number of Al, greater acidity for isomerization, greater *p*/*o* -*m*-Xylene conversion = 7%, *p*/*o* ~1.18	350	Greater number of Al, greater acid site, 0–1000 μmol/g for number of Al = 0–40	[72]

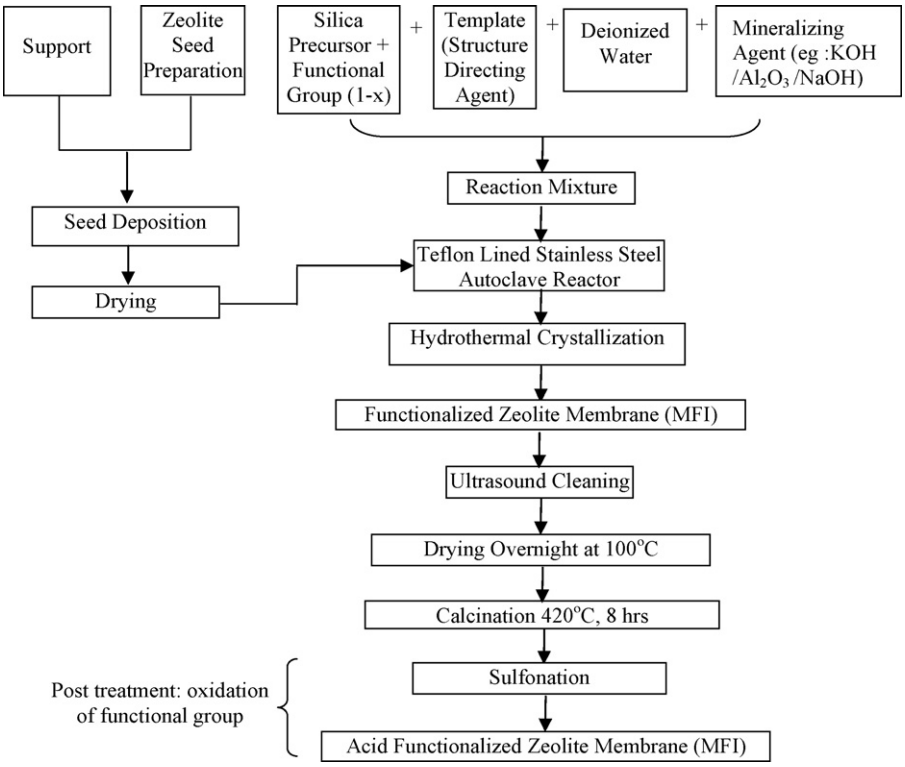

Fig. 7. Combination of secondary growth and in situ deposition method for synthesis of functionalized zeolite membrane.

logue of ZSM-5 (MFI) which is catalytically inactive in its pure form. Therefore, silicalite-1 zeolite membrane can be performed as an acid catalyst by introducing an organic functional group into the zeolite pores, which subsequently oxidized to acid, to produce acid-functionalized silicalite-1 zeolite membrane. The deposition of the acid-functional group into the zeolite pores will result in partial pore blocking of the pores, which is a great advantages for the enhanced selectivity and catalytic activity based on shape selectivity for combined xylene separation and isomerization.

By utilizing the methods used for synthesis of zeolite MFI membrane and functionalized zeolite materials, a new method for development of functionalized MFI zeolite membrane has been proposed (Fig. 7). Fig. 8 shows the conceptual diagram of acid-functionalized zeolite MFI membrane as a separator and catalyst for combined reaction and separation of xylenes. In order to achieve excellent performance in combined reaction and separation for xylene isomerization, high quality acid-functionalized zeolite membrane is needed. It is very important for acid-functional group to be deposited in the micropores of the zeolite in order to perform as shape-selective catalyst in xylene isomerization. The optimum composition and the type of the functional group deposited in the zeolite pores need to be investigated, for optimum performance of the catalytic membrane reactor in the role of catalysis and separation. Thus, further studies and investigation are needed.

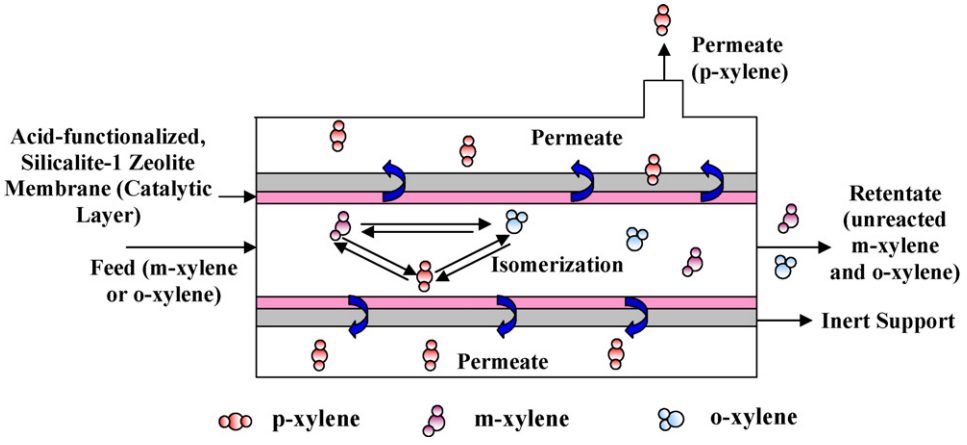

Fig. 8. Conceptual diagram of reactor using functionalized zeolite MFI membrane for combined xylenes isomerization (reaction) and separation of *para*-xylene (single stage of operation).

7. Xylene isomerization in functionalized zeolite membrane reactor

7.1. Research issues

There are number research issues which need to be addressed for further studies of combined separation and reaction in acid-functionalized catalytic membrane reactor. These are

- orientation of MFI zeolite membrane: important for *para*-xylene separation;
- right pore size of the membrane: important for separation and reaction;
- functional group acidity and stability: important for xylene isomerization reaction;
- modeling and simulation combining separation and reaction in the catalytic membrane reactor: better understanding of the combined process and will help in the scale up of the process.

For successful implementation of this type of membrane reactor, there are three important steps involved:

(i) Synthesis of *b*-oriented MFI zeolite membrane.
(ii) Introduction of catalytic active sites (functional groups and subsequent oxidation to acid sites) into the membrane.
(iii) Simultaneous reaction and separation in catalytic zeolite membrane reactor for *para*-xylene production.

Therefore, the focus in this research area has been on the synthesis and characterization of acid-functionalized zeolite membrane and to study the catalytic activity of the functionalized zeolite membrane for maximum conversion and recovery of *para*-xylene from its isomers.

7.2. Vapor permeation catalytic membrane test rig

A vapor permeation membrane test rig could be used to test:

(i) The performance of the *b*-oriented MFI zeolite membrane in separation of vapor xylene mixtures.
(ii) The performance of *b*-oriented, acid-functionalized MFI zeolite membrane in combination of reaction and separation of xylene mixtures.

The schematic of the rig is shown in Fig. 9. It consists of feed tank, metering pump, heating system, furnace, disc type/tubular type membrane cell, back pressure regulator, liquid rotameter, mass flow controller and vacuum pump. In order to obtain the desired separation or combined separation and reaction data, the rig can be operated by setting the feed flow rate, temperature and pressure accordingly. Sample collected from permeate and retentate streams could be analyzed by an offline gas chromatograph (GC).

7.3. Important parameters and data analysis

- Separation performance studies
  The separation performance of *b*-oriented MFI zeolite membrane for single, binary mixtures and ternary mixtures of xylenes is evaluated by flux and separation factor.

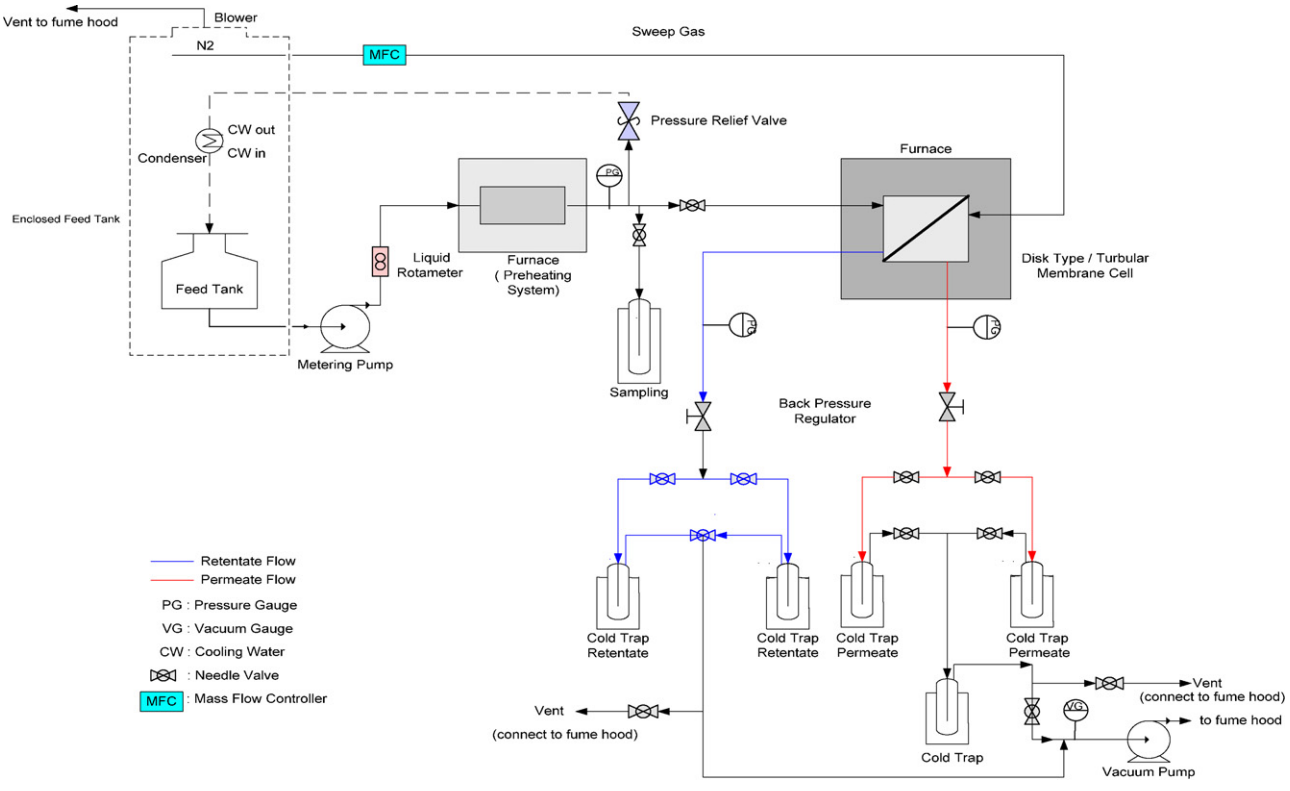

Fig. 9. Schematic of vapor permeation membrane test rig.

Flux is defined as

$$J_i = \frac{W_i}{At} \quad (1)$$

where J_i = permeation flux of the component i (kg/(m^2 s)); W_i = weight of the component i (kg); A = membrane area (m^2); t = operating time (s).

Separation factor is defined as

$$\alpha_{1/2} = \frac{y_1/y_2}{x_1/x_2} \quad (2)$$

where y_i = molar fraction of component i at permeate; x_i = molar fraction of component i at retentate; i = component 1 or component 2.

- Combined separation and reaction studies

  The *b*-oriented, acid-functionalized MFI zeolite membrane could be tested for its performance in combined separation and xylene isomerization reaction as a membrane test unit. The conversion and the *p*-xylene yield are evaluated in the process. The operating parameters are

  (i) Feed pressure of *m*-xylene or *o*-xylene ranging from 0.5 to 1.5 bar.
  (ii) Operating temperature ranging from 300 to 450 °C.
  (iii) Contact time (weight hourly space velocity, WHSV) ranging from 0.3 to 0.7 h^{-1}.
  (iv) Trans-membrane pressure ranging from 0.2 to 1 bar.

The conversion of xylene (*ortho* or *meta*) is defined as

$$X = \frac{(C_i)_{in} - (C_i)_{out}}{(C_i)_{in}} \quad (3)$$

where X = xylene conversion; $(C_i)_{in}$ = inlet molar flow/concentration of xylene; $(C_i)_{out}$ = outlet molar flow/concentration of xylene.

The *p*-xylene yield will be defined as

$$p\text{-xylene yield} = \frac{C^{Pr} + C^{Pp}}{C^{Pr} + C^{Pp} + C^{ir} + C^{ip}} \quad (4)$$

where C^{Pr} = concentration of *p*-xylene in retentate; C^{Pp} = concentration of *p*-xylene in permeate; C^{ir} = concentration of *o*-xylene or *m*-xylene in retentate; C^{ip} = concentration of *o*-xylene or *m*-xylene in permeate.

8. Mathematical model for combined separation and isomerization

8.1. Separation properties for zeolite membrane

Separations using zeolite membranes are due to the result of a combination of differences in diffusivities and preferential adsorption, and separations can favor either the more mobile or the more strongly adsorbing component [73]. The permeation flux of a component is determined by the adsorption and diffusion characteristics of all of the components in the mixture, and separation characteristics cannot be estimated from single component permeation data alone. The proper description of mass transport or permeation in zeolite membrane must take account of the subtle interplay between adsorption and diffusion, and also coupling between species diffusion [74]. The mass transport in microporous materials generally, governed by surface diffusion. Therefore, the understanding of sorption and diffusion in these materials is of fundamental interest and important for the understanding of the shape-selective catalytic and separation characteristics of zeolites. Among the different models for diffusion in zeolite membrane currently used, surface diffusion is the dominant transport mechanism for zeolite membranes, where molecules adsorb on the feed side surface, diffuse from one adsorption site to the next with the net diffusion in the direction of decreasing chemical potential, and desorb from the zeolite on the permeate side. Flow through the porous support is a combination of bulk diffusion, Knudsen diffusion and viscous flow [73].

Van Den Broeke et al. [75], Jeong et al. [23] and Van De Graaf et al. [76] reported that the mass transport through the zeolite membrane follows:

(i) adsorption from the feed on the external surface of the membrane;
(ii) transport or diffusion from the external surface in to the membrane pores;
(iii) intracrystalline transport;
(iv) transport from the membrane pores to the external surface;
(v) desorption from the external surface of the membrane at the permeate side.

A schematic represent the mass transport through zeolite membrane is shown in Fig. 10 [77].

8.1.1. Adsorption model

For the description of the equilibrium adsorption in zeolites membrane, various models have been successfully applied to describe the isotherms for single component, binary mixture and multicomponents. This includes:

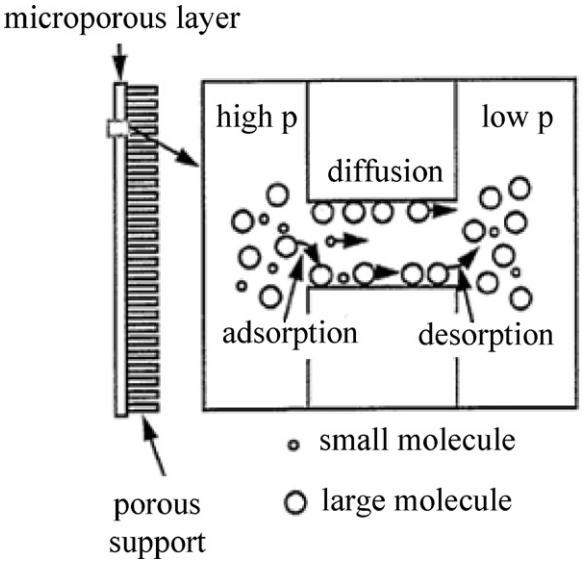

Fig. 10. Schematic showing the mass transport through zeolite membrane [77].

- Langmuir isotherm;
- dual site Langmuir (DSL) isotherm;
- extended or multicomponent Langmuir isotherm;
- ideal adsorbed sorption theory (IAST);
- real adsorbed sorption theory (RAST).

Krishna et al. [77–80] modeled permeation of single component and binary mixtures using both single and dual site Langmuir isotherm for hydrocarbons. Extended Langmuir isotherm was used for the two-component system. The extended Langmuir isotherm is a good representation when the saturation loadings of the two components are same. When the saturation loadings differ significantly, the extended Langmuir isotherms do not predict observed behavior, particularly at high occupancies, where the component with higher saturation loading can dominate adsorption [73]. Therefore, ideal adsorbed sorption theory (IAST) [75,78,81] and real adsorbed sorption theory (RAST) [78,82] were used to predict the adsorption behaviors of the mixtures. Fig. 11 shows the simulated results obtained by Krishna and Paschek [78] for single component and binary mixture of *n*-hexane and 2,2-dimethylbutane in silicalite membrane. The experiment data fitted well with the selected adsorption models.

8.1.2. Diffusion model

The Maxwell–Stefan formulation, theoretical model of surface diffusion has been studied extensively and successfully applied for the description of single component permeation and the quantitative prediction of binary permeation through a microporous inorganic membrane (silicalite-1 membrane) by Krishna et al. [78–81,83–87]. The general Maxwell Stefan equation for a binary mixture is given as

$$(N) = -\rho_Z[\Theta_{\text{sat}}][B]^{-1}[\Gamma]\nabla(\theta) \tag{5}$$

where $[\Theta_{\text{sat}}]$ is a diagonal matrix with the saturation loadings $\Theta_{i,\text{sat}}$ with i = component 1 or component 2. $[B]$ is the square matrix of inverse Maxwell–Stefan coefficients. $[\Gamma]$ is matrix of thermodynamic factors and $\nabla\theta$ is gradient of fractional loading. The model has been successfully used to predict the selectivity of hydrocarbon mixtures permeating through zeolite membranes using known properties of zeolites. The Maxwell–Stefan formulation is indispensable for the description

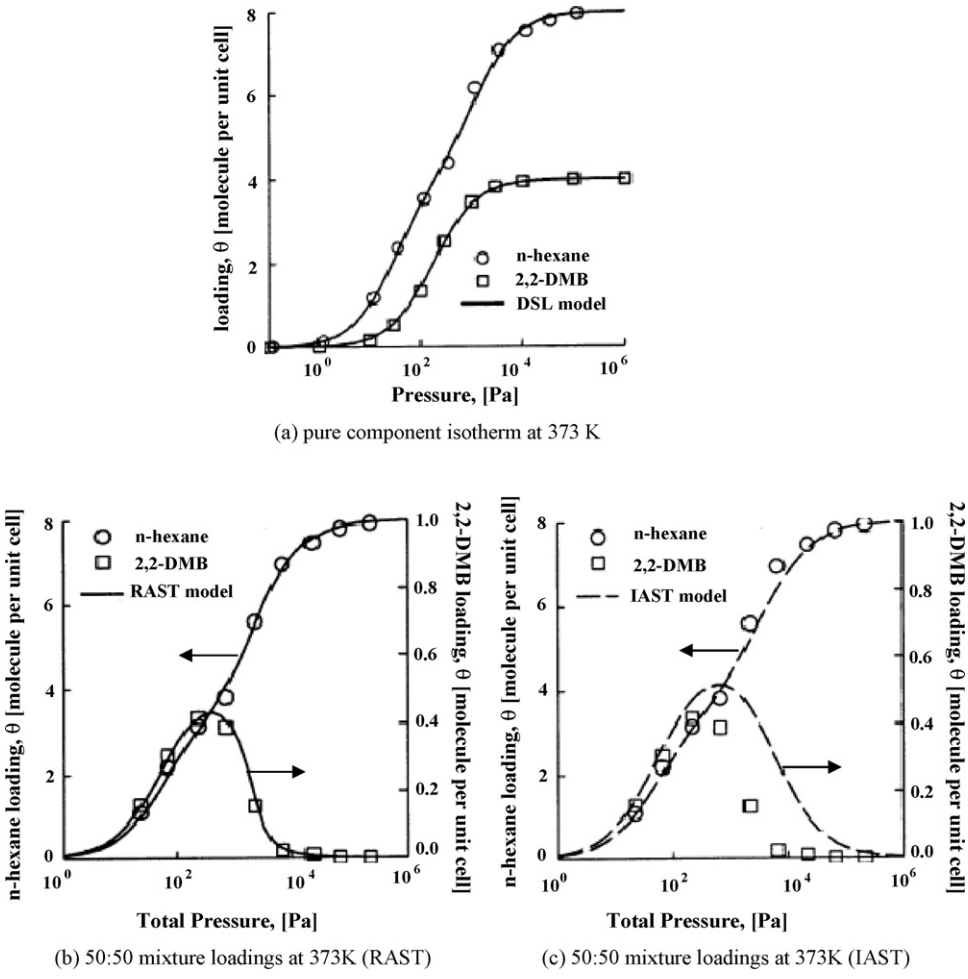

(a) pure component isotherm at 373 K

(b) 50:50 mixture loadings at 373K (RAST)

(c) 50:50 mixture loadings at 373K (IAST)

Fig. 11. Simulated results obtained by Krishna and Paschek [78] for single component (a) and binary mixture (b and c) of *n*-hexane and 2,2-dimethylbutane in silicalite membrane.

of mass transport across zeolite membrane. Krishna and Paschek [80] compared the single and binary mixture of *n*-hexane and 2,2-dimethylbutane experimental data with simulated results obtained using Eq. (5) and found that these results fitted well with the experimental data.

8.1.3. Separation factor

For pure component, the sorption selectivity in the mixture is defined as [78,88]

$$\text{sorption selectivity} = \frac{\Theta_1/\Theta_2}{p_1^r/p_2^r} \quad (6)$$

Θ_i is refer to the molecular loadings of the pure component in the mixture within the zeolite Both differences in the saturation capacities and molecular configurations are important factors of the sorption selectivity in the mixture.

For a binary mixture, the separation factor for the zeolite membrane is calculated from the ratio of the binary permeances. The steady-state selectivity is defined as [78,88]

$$\text{permeation selectivity} = \frac{N_2/N_1}{p_2^p/p_1^p} \quad (7)$$

Maxwell–Stefan theory may possible to describe the diffusion behavior of xylene mixture through zeolite membrane. A suitable adsorption isotherm needs to be found to adequately describe the adsorption behavior of the xylene mixtures. The combination of adsorption isotherm and Maxwell–Stefan equations are possibly adequate to describe the permeation behavior of single, binary as well as ternary mixture of xylene through the catalytic zeolite membrane.

8.2. Mathematical model for xylene isomerization

There is a need for a detailed theoretical model (reaction and diffusional transport) that can help in the understanding the performance, potentialities and the limitations of the separation and xylene isomerization reaction on catalytic zeolite layer in a catalytic membrane reactor. The reaction scheme of xylene isomerization over acid catalysts has been an issue of controversy over the years. In the literature, two different models have been employed for kinetic studies to describe xylene isomerization (by ignoring disproportionation reaction): a general triangular scheme (Fig. 12a) for the three xylenes and a simple linear scheme (Fig. 12b) in which the reaction is assumed to proceed via intramolecular 1,2-shifts of the methyl groups. The latter allows transformation of *o*- into *p*-xylene (and vice versa) only through *m*-xylene as an intermediate step, but not directly. Both schemes have been used by different researchers for the modeling of xylene isomerization using zeolite catalyst [89].

In order to describe the isomerization of xylene mathematically, a diffusion–reaction model with a sequential reaction scheme have been applied by Hedlund et al. [68] to model their experiment data of xylene isomerization over thin ZSM-5 film. According to them, xylene isomerization was modeled as a series of first-order reversible reactions. However, they claimed

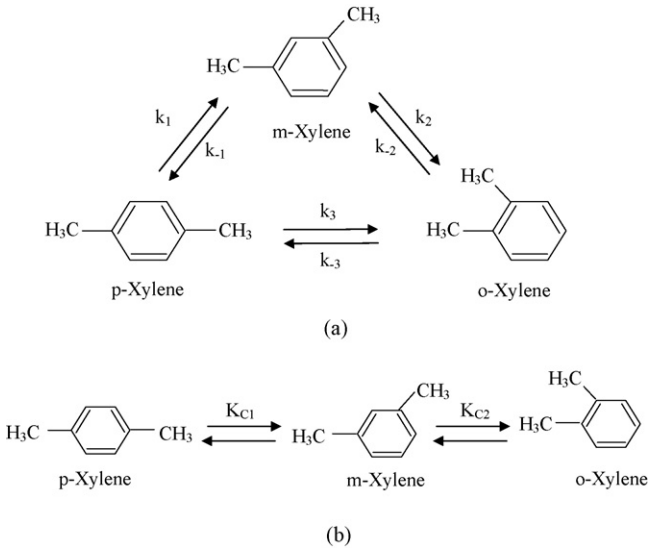

Fig. 12. (a) Triangular reaction scheme of xylene isomerization [67] and (b) linear or sequence reaction scheme of xylene isomerization [68].

that, under strong mass transfer control, the system follows an apparent triangular reaction scheme.

Kinetics of xylene isomerization on the catalytically active H-ZSM-5 membrane has been studied by Stephane Haag et al. [67], for reaction and separation of *p*-xylene from the other isomers. They reported that the reaction kinetics was best described by a general triangular scheme. Based on the experimental data in their study, they found that the linear scheme systematically underestimated the yield of *o*-xylene from pure *p*-xylene feeds and vice versa; the simulation was consistent with the experimental data only for *m*-xylene as the feed. Therefore, the triangular reaction scheme was adopted.

8.3. Modeling of functionalized catalytic membrane reactor

In order to optimize conversion, yield, flux and *p*-xylene separation, a suitable process model represents the xylene isomerization over the acid-functionalized MFI zeolite membrane together with the continuous separation of *p*-xylene through the acid-functionalized MFI zeolite membrane need to be developed. This process model will be very useful in the rational design of catalytic membrane reactor unit for reaction and separation of *p*-xylene in a single unit.

During the past few years, there have been a number of studies reported about the modeling of the catalytic membrane reactors. A mathematical model for the methane reforming reaction was developed by Prabhu et al. [90] to simulate the performance of the membrane reactors. Jeong et al. [91] conducted a mathematical analysis to evaluate the performance of a FAU-type membrane reactor use for the catalytic dehydrogenation of cyclohexane. Their model prediction and simulation results were in good agreement with the experimental data. Experimental and modeling study of catalytic membrane reactor has been performed by Bottino et al. [92] for the oxydehydrogenation of propane. The compatibility between the model and the experimental data was verified for all the operative conditions

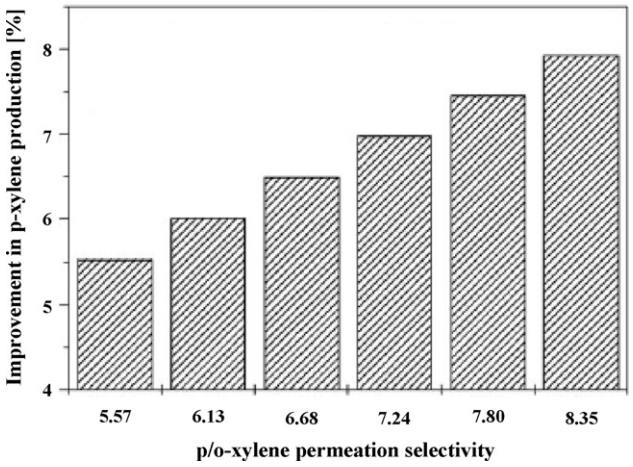

Fig. 13. Simulated results: influence of *p*-/*o*-xylene permeation selectivity in the production of *p*-xylene [10].

studied and they found that the use of a thicker catalytic layer can enhance the selectivity to propylene.

Recently, a model and the simulation of ZSM-5 membrane reactor containing catalyst for xylene isomerization were presented by Deshayes et al. [10]. The conventional plug-flow model was modified and the kinetic parameters were optimized to simulate the behavior of membrane reactor under industrial conditions. They found that the permeation area, sweep gas flow rate and residence time significantly influenced the *p*-xylene production. The influence of *p*-/*o*-xylene permeation selectivity in the production of *p*-xylene, obtained by Deshayes et al. [10] is presented in Fig. 13. Their simulation results predicted that increases in *p*-xylene production as high as 12% can be achieved in a ZSM-5 membrane reactor.

The work done by Deshayes et al. [10], Prabhu et al. [90] and Stephane Haag et al. [67] could be extended to a mathematical model for functionalized (catalytic) zeolite membrane in xylene isomerization. Fig. 14 shows the schematic of the functionalized catalytic zeolite membrane reactor. The following assumptions are applied in the development of the model [90–93]:

(i) xylene disproportionation is neglected;
(ii) steady-state and isothermal operation;
(iii) the flow pattern for the retentate and permeate streams is considered to be plug flow;
(iv) constant diffusion and sorption coefficients;
(v) negligible pressure's drop along the retentate and permeate sides;
(vi) elementary reaction mechanism;
(vii) homogeneous catalyst distribution through the membrane;
(viii) the reaction occurs only on the catalytic membrane surface;
(ix) equal concentration of reactant on the catalyst surface in the catalytic membrane.

The reactor performance, in terms of the conversion enhancement over a thermodynamic equilibrium could be analyzed based on the influence of the relative sorption, diffusion coefficients and operation parameters of the reaction components. The mathematical model comprises the steady-state mass balance equations for the retentate and permeate sides as well as the respective boundary conditions, are used as a basic equations to study the reactor performance [90,67]. Refer to Fig. 14, the equations are represented as

- Mass balance

For steady-state operation:

$$\text{input} - \text{output} + \text{generation} = 0$$

(1) Mass balance in the retentate side:

$$\frac{dN_i^r}{dz} + 2\frac{D_i H_i R_1 (P_i^p - P_i^r)}{R_1} - \nu_i r_i = 0 \quad (8)$$

$i = m$-xylene, o-xylene, p-xylene.

The boundary conditions areAt $z = 0$, $P_i^r = P_i^f$.

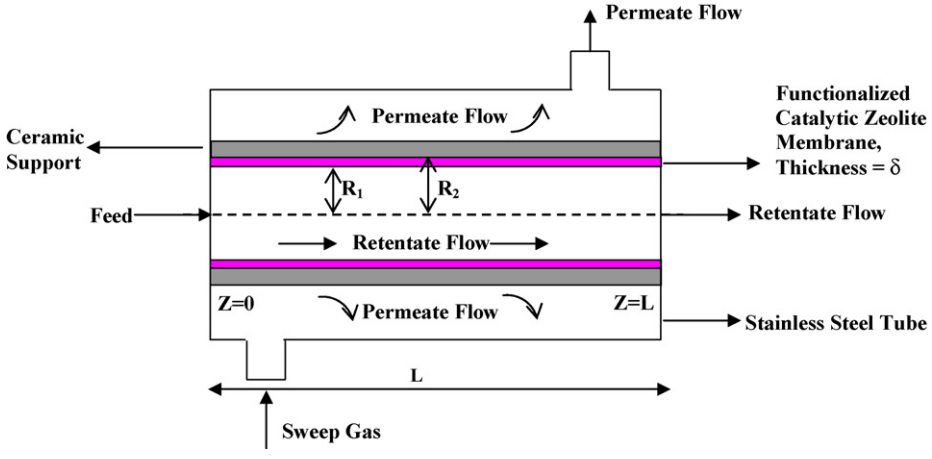

Fig. 14. Schematic of the functionalized catalytic membrane reactor.

(2) Mass balance in the permeate side:

$$\frac{dN_i^p}{dz} - \frac{2D_i H_i R_1 (P_i^p - P_i^r)}{R_2^2 - R_1^2} = 0 \quad (9)$$

The boundary conditions are:At $z=0$, $P_i^p(z) = 0$.

P_i^f, P_i^r and P_i^p represent the partial pressure of species i in feed, retentate and permeate streams, respectively. N_i^p and N_i^r are molar flux of species i in retentate and permeate streams, respectively. R_1 is the membrane radius on the retentate side; $R_2 - R_1$ is the membrane radius on the permeate side. z the axial coordinate along the reactor length and r_i is rate of reaction; $D_i\psi$ and $H_i\psi$ are the diffusion and sorption coefficients of component i; $v_i\psi$ is the stoichiometric coefficient of component. The partial pressure of each component can be evaluated as

- Retentate side:

$$p_i^r = x_i P = \frac{Q_i^r}{\sum Q_i^r} P \quad (10)$$

- Permeate side:

$$p_i^p = y_i P = \frac{Q_i^p}{\sum Q_i^p} P \quad (11)$$

P is the total pressure; Q_i^r and Q_i^p are the volumetric flowrate of species i in retentate and permeate stream.

Assuming the xylene isomerization reaction in functionalized catalytic membrane reactor is controlled by mass transfer, the triangular scheme kinetic model can be applied to represent xylene isomerization reaction (as shown in Fig. 12a). Xylene isomerization is modeled as a series of first-order reversible reaction and the rates of formation r_i are written as first-order reaction:

$$r_P = -\frac{k_1}{\rho_z}\left(C_P - \frac{C_M}{K_{C_1}}\right) - \frac{k_3}{\rho_Z}\left(C_P - \frac{C_O}{K_{C_3}}\right) \quad (12)$$

$$r_M = \frac{k_1}{\rho_z}\left(C_P - \frac{C_M}{K_{C_1}}\right) - \frac{k_2}{\rho_Z}\left(C_M - \frac{C_O}{K_{C_2}}\right) \quad (13)$$

$$r_O = \frac{k_2}{\rho_z}\left(C_M - \frac{C_O}{K_{C_2}}\right) + \frac{k_3}{\rho_Z}\left(C_P - \frac{C_O}{K_{C_3}}\right) \quad (14)$$

where $K_{C_1} = k_1/k_{-1}$, $K_{C_2} = k_2/k_{-2}$, $K_{C_3} = k_3/k_{-3}$, $k_i = k_{io}\exp(-E_i/\Re T)$, ρ_Z is density of zeolite and C_P, C_M, C_O = concentration of *p*-xylene, *m*-xylene and *o*-xylene, respectively. K_i is equilibrium constant, k_i is the rate constant and k_{io} is Arrhenius prefactor. The equilibrium constants are calculated from thermodynamic data assuming ideal vapor phase.

Fig. 15 shows the flow chart in development of mathematical model for combined separation and xylene isomerization over functionalized catalytic zeolite membrane. The effect of parameters such as sorption and diffusion coefficients, molecular sieving effect, membrane area, temperature, pressure, reaction contact time, amount of catalyst used, length of the membrane and sweep gas flow need to be considered in the equations. Conversion, yield, flux and selectivity for *p*-xylene could be calculated from the model using simulation. The simulation results could be compared with the experimental data in order to verify the kinetic model developed.

9. Future perspective for functionalized zeolite membrane

Functionalized zeolite membranes are a new type of membrane materials which have a large potential not only as a shape-selective catalyst in combined xylene isomerization and separation, but also for other applications depending on the functional groups introduced into the zeolite pore structure. New avenues and research directions have been suggested by developing this type of membranes by using a right kind of functional groups for specific applications.

Acid-functionalized zeolite membrane can be applied as catalytic membrane reactor for other acid-catalyzed reaction such as methanol to olefin [94], to improve the selectivity of olefins in the methanol conversion by controlling the location of the acid sites. By utilizing of acid-functionalized catalytic membrane reactor, the conversion of CO_2 hydrogenation into methanol may also be improved [95]. By deposition of the right kind of functional group into the zeolite membrane, it also can be applied as a catalyst for water-gas-shift (WGS) reaction to improve the selectivity for H_2 production [96]. However, the application of functionalized zeolite membrane in these types of reaction still needs to be studied.

For zeolite-based sensors application, the development of functionalized zeolite membrane can be used to improve the catalytic and filtering properties of the sensors, for e.g., catalytic reduction of NOx. The better sensitivity and selectivity of the sensor will effectively measure and control the emission gases from power plants, chemical plants and motor vehicles, for the purpose to improve the air quality in the atmosphere. Since the catalytic reduction of combustion gases involved high temperature, the thermal stability of the membrane still needs to be investigated [97,98].

McLeary et al. [99] reported that "ultramicroporous" membranes, i.e. those with sufficiently small pores (~0.3 nm) to allow separation on the basis of size exclusion or molecular sieving effect, and not only depending on preferential adsorption and diffusion, still not been developed yet. The majority of the membranes synthesized have pore diameters (~0.5 nm), which are still too big to selectively separate small gaseous molecules. Functionalized zeolite membranes are categories as ultramicroporous membrane because of its zeolite pore structure are partially blocked by functional groups. Therefore, it can also be used to selectively separate small gaseous molecules based on molecular sieving effects.

There is a scope of further studies in order to develop an appropriate functionalized zeolite membrane for different types of catalyzed reaction with the choice of functional group. The application of these membranes will open new type of separators based on size exclusion principle specially with ultramicroporous zeolite membrane.

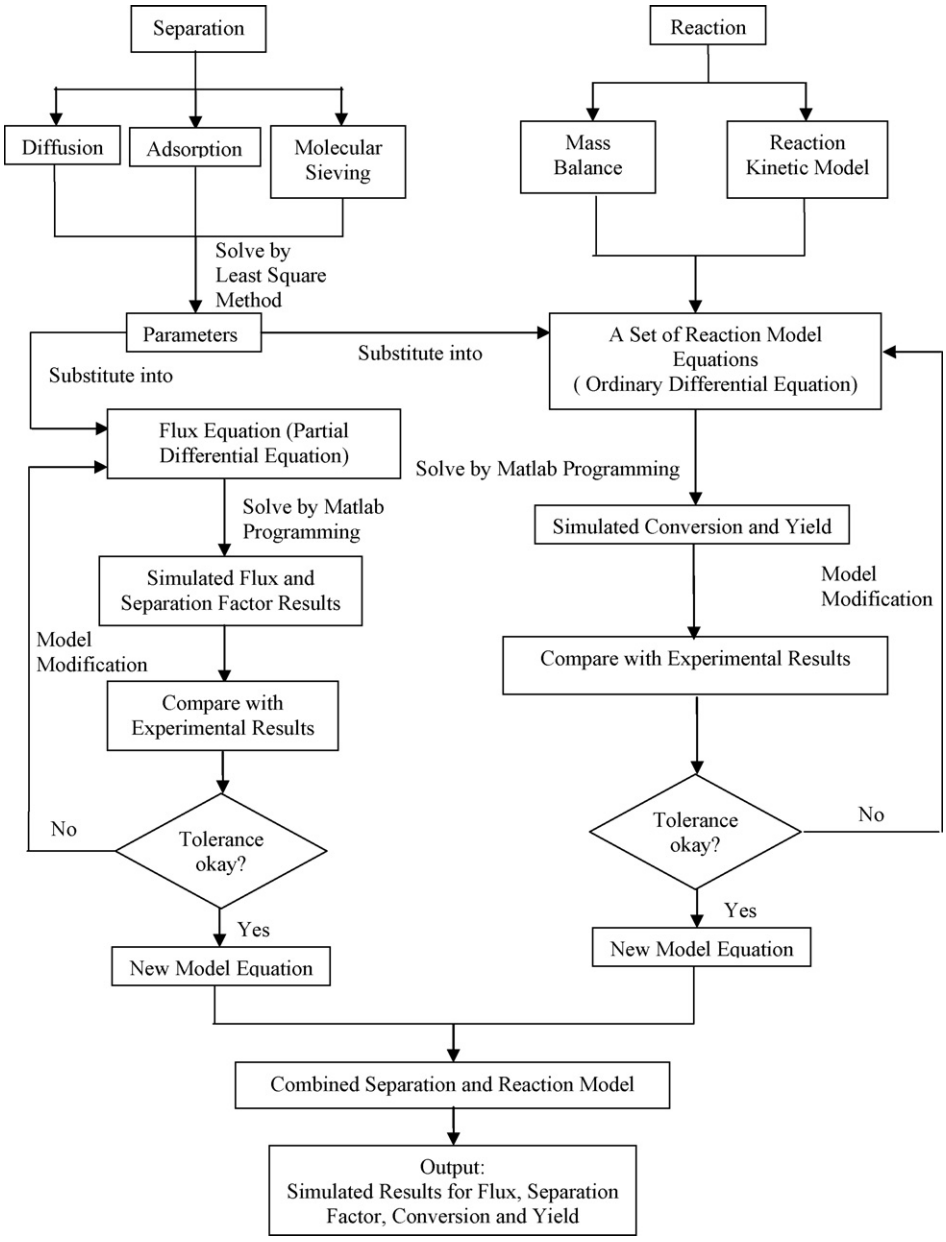

Fig. 15. Flow chart showing the development of mathematical modeling for combined separation and xylene isomerization over functionalized catalytic zeolite membrane.

10. Concluding remarks

The development of functionalized zeolite membrane has been suggested in the present review; however, there are still many challenging issues. The crystallinity, orientation, acidity, pore size and thermal stability of the organic–inorganic hybrid membrane need to be figured out. Besides of its potential application as a catalytic membrane for combined xylene separation and isomerization, its potential applications in other type of systems should also be considered. For the propose of design and scale up, mathematical models are useful to understand the simultaneous role of the membrane in the catalysis as well as separation process. The successful implementation of the catalytic functionalized membrane may result in substantial energy and cost saving in the industry.

Acknowledgements

The financial support provided by Universiti Sains Malaysia under Short Term Grant (Account No.: 6035188) Fundamental Research Grant Scheme (FGRS, Account No.: 6070021) and eScience Fund Grant (Account No.: 6013319) are duly acknowledged.

References

[1] Z. Lai, G. Bonilla, I. Diaz, J.G. Nery, K. Sujaoti, M.A. Amat, E. Kokkoli, O. Terasaki, R.W. Thompson, M. Tsapatsis, D.G. Vlachos, Science 300 (2003) 456–460.
[2] G. Xomeritakis, Z. Lai, M. Tsapatsis, Ind. Eng. Chem. Res. 40 (2001) 544–552.
[3] C.Y. Tsai, S.Y. Tam, Y. Lu, C.J. Brinker, J. Membr. Sci. 169 (2000) 255–268.

[4] H. Sakai, T. Tomita, T. Takahashi, Sep. Purif. Technol. 25 (2001) 297–309.
[5] T. Matsufuji, N. Nishiyama, M. Matsukata, K. Ueyama, J. Membr. Sci. 178 (2000) 25–34.
[6] J. Motuzas, A. Julbe, R.D. Noble, C. Guizard, Z.J. Beresnevicius, D. Cot, Micropor. Mesopor. Mater. 80 (2005) 73–83.
[7] W. Shan, Y. Zhang, W. Yang, C. Ke, Z. Gao, Y. Ye, Y. Tang, Micropor. Mesopor. Mater. 69 (2004) 35–42.
[8] M.P. Bernal, G. Xomeritakis, M. Tsapatsis, Catal. Today 67 (2001) 101–107.
[9] G. Bonilla, D. Vlachos, M. Tsapatsis, Micropor. Mesopor. Mater. 42 (2001) 191–203.
[10] A.L. Deshayes, E.E. Miro, G.I. Horowitz, Chem. Eng. J. 122 (2006) 149–157.
[11] J. Hedlund, J. Sterte, M. Anthonis, A. Bons, B. Carstensen, N. Corcoran, D. Cox, H. Deckman, W. Gijnst, P. Moor, F. Lai, J. Mchenry, W. Mortier, J. Reinoso, J. Peters, Micropor. Mesopor. Mater. 52 (2002) 179–189.
[12] H. Kita, K. Fuchida, T. Horita, H. Asamura, K. Okamoto, Sep. Purif. Technol. 25 (2001) 261–268.
[13] S. Nair, Z. Lai, V. Nikolakis, G. Xomeristakis, G. Bonilla, M. Tsapatsis, Micropor. Mesopor. Mater. 48 (2001) 219–228.
[14] Z. Lai, M. Tsapatsis, Ind. Eng. Chem. Res. 43 (2004) 3000–3007.
[15] K. Keizer, A.J. Burggraaf, Z.A.E.P. Vroon, H. Verweij, J. Membr. Sci. 147 (1998) 159–172.
[16] C.J. Gump, V.A. Tuan, R.D. Noble, J.L. Falconer, Ind. Eng. Chem. Res. 40 (2001) 565–577.
[17] O. De La Iglesia, S. Irusta, R. Mallada, M. Menendez, J. Coronas, J. Santamaria, Micropor. Mesopor. Mater. 93 (2006) 318–324.
[18] X. Cheng, Z. Wang, Y. Yan, Electrochem. Solid-State Lett. 4 (2001) 23–26.
[19] A.M.P. McDonnell, D. Beving, A. Wang, W. Chen, Y. Yan, Adv. Funct. Mater. 15 (2005) 336–340.
[20] Ch. Baerlocher, W.M. Meier, D.H. Olson, Atlas of Zeolite Framework Types, 5th ed., Structure Commission of the International Zeolite Association, Elsevier, Amsterdam, 2001.
[21] L. Dyk, L. Lorenzen, S. Miachon, J. Dalmon, Catal. Today 104 (2005) 274–280.
[22] J. Hedlund, M. Noack, P. Kolsch, D. Creaser, J. Caro, J. Sterte, J. Membr. Sci. 159 (1999) 263–273.
[23] B.H. Jeong, Y. Hasegawa, K. Sotowa, K. Kusakabe, S. Morooka, J. Membr. Sci. 213 (2003) 115–124.
[24] V. Nikolakis, G. Xomeritakis, A. Abibi, M. Dickson, M. Tsapatsis, D.G. Vlachos, J. Membr. Sci. 184 (2001) 209–219.
[25] C.W. Jones, Science 300 (2003) 439–440.
[26] C.W. Jones, K. Tsuji, M.E. Davis, Micropor. Mesopor. Mater. 33 (1999) 223–240.
[27] C.W. Jones, M. Tsapatsis, O. Tatsuya, M.E. Davis, Micropor. Mesopor. Mater. 42 (2001) 21–35.
[28] K. Tsuji, C.W. Jones, M.E. Davis, Micropor. Mesopor. Mater. 29 (1999) 339–349.
[29] S. Monique, G. Elisabeth, O.G. Jean, P.V. Valentin, J. Mater. Chem. 14 (2004) 1347–1351.
[30] B.A. Holmberg, S.J. Hwang, M.E. Davis, Y. Yan, Micropor. Mesopor. Mater. 80 (2005) 347–356.
[31] Y. Shin, S.Z. Thomas, E.F. Glen, L.Q. Wang, L. Jun, Micropor. Mesopor. Mater. 37 (2000) 49–56.
[32] I.K. Mbaraka, D.R. Radu, S.Y. Lin, B.H. Shanks, J. Catal. 219 (2003) 329–336.
[33] E. Kikuchi, K. Yamashita, S. Hitomoto, K. Ueyama, M. Matsukata, Micropor. Mesopor. Mater. 11 (1997) 107–116.
[34] W. Yuan, Y.S. Lin, W. Yang, J. Am. Chem. Soc. 126 (2004) 4776–4777.
[35] L.T.Y. Au, W.Y. Mui, P.S. Lau, C.T. Ariso, K.L. Yeung, Micropor. Mesopor. Mater. 47 (2001) 203–216.
[36] G. Li, E. Kikuchi, M. Matsukata, Micropor. Mesopor. Mater. 62 (2003) 211–220.
[37] M.C. Lovallo, M. Tsapatsis, AIChE 42 (1996) 3020–3029.
[38] M.C. Lovallo, M. Tsapatsis, T. Okubo, Chem. Mater. 8 (1996) 1579–1583.
[39] J. Motuzas, A. Julbe, R.D. Noble, A. Van Der Lee, Z.J. Beresnevicius, Micropor. Mesopor. Mater. 92 (2006) 259–269.
[40] A. Huang, Y.S. Lin, W. Yang, J. Membr. Sci. 245 (2004) 41–51.
[41] M. Abdollahi, S.N. Ashrafizadeh, A. Malekpour, Micropor. Mesopor. Mater. 106 (2007) 192–200.
[42] M.J. Exter, H. Bekkum, C.J.M. Rijn, F. Kapteijn, J.A. Moulijn, H. Schellevis, C.I.N. Beenakker, Zeolites 19 (1997) 13–20.
[43] J.S. Lee, Y.J. Lee, E.L. Tae, S.P. Yong, K.B. Yoon, Science 301 (2003) 818–821.
[44] A. Bons, P.D. Bons, Micropor. Mesopor. Mater. 62 (2003) 9–16.
[45] Z. Wang, Y. Yan, Micropor. Mesopor. Mater. 48 (2001) 229–238.
[46] J.H. Koegler, H. Bekkum, J.C. Jansen, Zeolites 19 (1997) 262–269.
[47] W.Y. Dong, Y.C. Long, Micropor. Mesopor. Mater. 76 (2004) 9–15.
[48] G. Xomeritakis, S. Naik, C.M. Braunbarth, C.J. Cornelius, R. Pardey, C.J. Brinker, J. Membr. Sci. 215 (2003) 225–233.
[49] H. Yu, X. Wang, Y. Long, Micropor. Mesopor. Mater. 95 (2006) 235–241.
[50] A.M. Tarditi, S. Irusta, E.A. Lombardo, Chem. Eng. J. 122 (2006) 167–174.
[51] G.T.P. Mabande, S. Ghosh, Z. Lai, W. Schwieger, M. Tsapatsis, Ind. Eng. Chem. Res. 44 (2005) 9086–9095.
[52] G.T.P. Mabande, G. Pradhan, W. Schwieger, M. Hanebuth, R. Dittmeyer, T. Selvam, A. Zampieri, H. Baser, R. Herrmann, Micropor. Mesopor. Mater. 75 (2004) 209–220.
[53] G. Xomeritakis, A. Gouzinis, S. Nair, T. Okubo, M. He, R.M. Overney, M. Tsapatsis, Chem. Eng. Sci. 54 (1999) 3521–3531.
[54] K. Wegner, J. Dong, Y.S. Lin, J. Membr. Sci. 158 (1999) 17–27.
[55] G. Xomeritakis, S. Nair, M. Tsapatsis, Micropor. Mesopor. Mater. 38 (2000) 61–73.
[56] X. Gu, J. Dong, T.M. Nenoff, D.E. Ozokwelu, J. Membr. Sci. 280 (2006) 624–633.
[57] X. Wang, J.C.C. Chan, Y.H. Tseng, S. Cheng, Micropor. Mesopor. Mater. 95 (2006) 58–66.
[58] U. Diaz, A. Jose, V. Moya, A. Corma, Micropor. Mesopor. Mater. 93 (2006) 180–189.
[59] J. Guo, A.J. Han, H. Yu, J.P. Dong, H. He, Y.C. Long, Micropor. Mesopor. Mater. 94 (2006) 166–172.
[60] K. Yamamoto, Y. Sakata, Y. Nohara, Y. Takahashi, T. Tatsumi, Science 300 (2003) 470–472.
[61] M. Guisnet, N.S. Gnep, S. Morin, Micropor. Mesopor. Mater. 35-36 (2000) 47.
[62] S. Morin, N.S. Gnep, M. Guisnet, J. Catal. 159 (1996) 296–304.
[63] S. Morin, P. Ayrault, S.E. Mouahid, N.S. Gnep, M. Guisnet, Appl. Catal. A: Gen. 159 (1997) 317–331.
[64] S. Morin, N.S. Gnep, M. Guisnet, Appl. Catal. A: Gen. 168 (1998) 63–68.
[65] Y.G. Li, H. Jun, Appl. Catal. A: Gen. 142 (1996) 123–137.
[66] S. Al-Khattaf, A. Iliyas, A. Al-Amer, T. Inui, J. Mol. Catal. A: Chem. 225 (2005) 117–124.
[67] M. Stephane Haag, G.T.P. Hanebuth, A. Mabande, W. Avhale, R. Schwieger, Dittmeyer, Micropor. Mesopor. Mater. 96 (2006) 109–117.
[68] J. Hedlund, O. Ohrman, V. Msimang, E. Van Steen, W. Bohringer, S. Sibya, K. Moller, Chem. Eng. Sci. 59 (2004) 2647–2657.
[69] F. Bauer, E. Bilz, A. Freyer, Appl. Catal. A: Gen. 289 (2005) 2–9.
[70] K. Pamin, A. Kubacka, Z. Olejniczak, J. Haber, B. Sulikowski, Appl. Catal. A: Gen. 194–195 (2000) 137–146.
[71] S. Zheng, A. Jentys, J.A. Lercher, J. Catal. 241 (2006) 304–311.
[72] S. Morin, P. Ayrault, N.S. Gnep, M. Guisnet, Appl. Catal. A: Gen. 166 (1998) 281–292.
[73] J.G. Martinek, T.Q. Gardner, R.D. Noble, J.L. Falconer, Ind. Eng. Chem. Res. 45 (2006) 6032–6043.
[74] R. Krishna, R. Baur, Chem. Eng. J. 97 (2004) 37–45.
[75] L.J.P. Van Den Broeke, W.J.W. Bakker, F. Kapteijn, J.A. Moulijn, Chem. Eng. Sci. 54 (1999) 245–258.
[76] J.M. Van De Graaf, F. Kapteijn, J.A. Moulijn, J. Membr. Sci. 144 (1998) 87–104.
[77] R. Krishna, L.J.P. Van Den Broeke, Chem. Eng. J. 57 (1995) 155–162.
[78] R. Krishna, D. Paschek, Sep. Purif. Technol. 21 (2000) 111–136.
[79] R. Krishna, T.J.H. Vlugt, B. Smit, Chem. Eng. Sci. 54 (1999) 1751–1757.
[80] R. Krishna, D. Paschek, Ind. Eng. Chem. Res. 39 (2000) 2618–2622.
[81] R. Krishna, S. Calero, B. Smit, Chem. Eng. J. 88 (2002) 81–94.
[82] G. Calleja, A. Jimenez, J. Pau, L. Dominguez, P. Perez, Gas Sep. Purif. 8 (1994) 247–256.
[83] R. Krishna, R. Baur, Sep. Purif. Technol. 33 (2003) 213–254.

[84] R. Krishna, D. Paschek, Chem. Eng. J. 85 (2002) 7–15.
[85] R. Krishna, D. Paschek, Chem. Eng. J. 87 (2002) 1–9.
[86] R. Krishna, Chem. Eng. J. 84 (2001) 207–214.
[87] R. Krishna, Chem. Phys. Lett. 326 (2000) 477–484.
[88] R. Krishna, Int. Commun. Heat Mass Transfer 28 (2001) 337–346.
[89] A. Iliyas, S. Al-Khattaf, Chem. Eng. J. 107 (2005) 127–132.
[90] A.K. Prabhu, A. Liu, L.G. Lovell, S.T. Oyama, J. Membr. Sci. 177 (2000) 83–95.
[91] B.H. Jeong, K.I. Sotowa, K. Kusakabe, Chem. Eng. J. 103 (2004) 69–75.
[92] A. Bottino, G. Capannelli, A. Comite, J. Membr. Sci. 197 (2002) 75–88.
[93] T. Brinkmann, S.P. Perera, W.J. Thomas, Chem. Eng. Sci. 56 (2001) 2047–2061.
[94] T. Tago, K. Iwakai, K. Morita, K. Tanaka, T. Masuda, Catal. Today 105 (2005) 662–666.
[95] F. Gallucci, L. Paturzo, A. Basile, Chem. Eng. Process. 43 (2004) 1029–1036.
[96] A. Brunetti, G. Barbieri, E. Drioli, K.-H. Lee, B. Sea, D.W. Lee, Chem. Eng. Process. 46 (2007) 119–126.
[97] W.L. Rauch, M. Liu, J. Mater. Sci. 38 (2003) 4307–4317.
[98] C. Pijolat, J.P. Viricelle, G. Tournier, P. Montmeat, Thin Solid Films 490 (2005) 7–16.
[99] E.E. Mcleary, J.C. Jansen, F. Kapteijn, Micropor. Mesopor. Mater. 90 (2006) 198–220.